

Trinuclear First Row Transition Metal Complexes of a Hexapyridyl, Trialkoxy 1,3,5-Triarylbenzene Ligand

Emily Y. Tsui, Jacob S. Kanady, Michael W. Day and Theodor Agapie

Division of Chemistry and Chemical Engineering, Arnold and Mabel Beckman Laboratories of Chemical Synthesis, California Institute of Technology, Pasadena, California 91125

Supporting Information

Experimental Details

General Considerations	S2
Synthetic Procedures	S2
Figure S1. ^1H NMR spectrum of H_3L	S5
Figure S2. ^{13}C NMR spectrum of H_3L	S5
Figure S3. ^1H NMR spectrum of $\text{LMn}_3(\text{OAc})_3$	S6
Figure S4. ^1H NMR spectrum of $\text{LFe}_3(\text{OAc})_3$	S6
Figure S5. ^1H NMR spectrum of $\text{LCo}_3(\text{OAc})_3$	S7
Figure S6. ^1H NMR spectrum of $\text{LNi}_3(\text{OAc})_3$	S7
Figure S7. ^1H NMR spectrum of $\text{LCu}_3(\text{OAc})_3$	S8
Figure S8. ^1H NMR spectrum of $\text{LZn}_3(\text{OAc})_3$	S8
Figure S9. ^{13}C NMR spectrum of $\text{LZn}_3(\text{OAc})_3$	S9

Magnetic Susceptibility Measurements

General Considerations	S10
-------------------------------	-----

Crystallographic Information

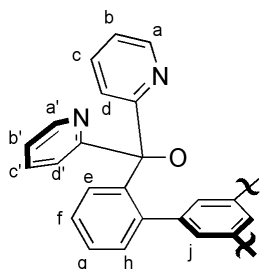
Table S1. Crystal and refinement data for $\text{LMn}_3(\text{OAc})_3$, $\text{LFe}_3(\text{OAc})_3$, $\text{LCo}_3(\text{OAc})_3$, $\text{LNi}_3(\text{OAc})_3$, $\text{LCu}_3(\text{OAc})_3$, and $\text{LZn}_3(\text{OAc})_3$	S10
Figure S10. Structural drawing of $\text{LMn}_3(\text{OAc})_3$	S11
Table S2. Atomic coordinates and equivalent isotropic displacement parameters for $\text{LMn}_3(\text{OAc})_3$	S12
Table S3. Anisotropic displacement parameters for $\text{LMn}_3(\text{OAc})_3$	S14
Figure S11. Structural drawing of $\text{LFe}_3(\text{OAc})_3$	S16
Table S4. Atomic coordinates and equivalent isotropic displacement parameters for $\text{LFe}_3(\text{OAc})_3$	S16
Table S5. Anisotropic displacement parameters for $\text{LFe}_3(\text{OAc})_3$	S18
Figure S12. Structural drawing of $\text{LCo}_3(\text{OAc})_3$	S20
Table S6. Atomic coordinates and equivalent isotropic displacement parameters for $\text{LCo}_3(\text{OAc})_3$	S21
Table S7. Anisotropic displacement parameters for $\text{LCo}_3(\text{OAc})_3$	S22
Figure S13. Structural drawing of $\text{LNi}_3(\text{OAc})_3$	S23
Table S8. Atomic coordinates and equivalent isotropic displacement parameters for $\text{LNi}_3(\text{OAc})_3$	S24
Table S9. Anisotropic displacement parameters for $\text{LNi}_3(\text{OAc})_3$	S24

Figure S14. Structural drawing of $\text{LCu}_3(\text{OAc})_3$	S25
Table S10. Atomic coordinates and equivalent isotropic displacement parameters for $\text{LCu}_3(\text{OAc})_3$	S26
Table S11. Anisotropic displacement parameters for $\text{LCu}_3(\text{OAc})_3$	S28
Figure S15. Structural drawing of $\text{LZn}_3(\text{OAc})_3$	S30
Table S12. Atomic coordinates and equivalent isotropic displacement parameters for $\text{LZn}_3(\text{OAc})_3$	S31
Table S13. Anisotropic displacement parameters for $\text{LZn}_3(\text{OAc})_3$	S32
References	S34

Experimental Details

General Considerations. Reactions performed under inert atmosphere were carried out in a glovebox under a nitrogen atmosphere. Anhydrous THF was purchased from Aldrich in 18 L Pure-PacTM containers. Anhydrous dichloromethane, acetonitrile, diethyl ether, and THF were purified by sparging with nitrogen for 15 minutes and then passing under nitrogen pressure through a column of activated A2 alumina (Zapp's). All non-dried solvents used were reagent grade or better. All NMR solvents were purchased from Cambridge Isotope Laboratories, Inc. CDCl_3 , CD_2Cl_2 , and CD_3CN were dried over calcium hydride, then degassed by three freeze-pump-thaw cycles and vacuum-transferred prior to use. ^1H NMR and ^{13}C NMR spectra were recorded on a Varian 300 MHz instrument or a Varian 500 MHz instrument, with shifts reported relative to the residual solvent peak. Elemental analyses were performed by Midwest Microlab, LLC, Indianapolis, IN. High resolution mass spectrometry data (HRMS) were obtained at the California Institute of Technology Mass Spectrometry Facility. UV-Vis spectra were taken on a Varian Cary 50 spectrophotometer using a quartz crystal cell.

Unless indicated otherwise, all commercial chemicals were used as received. Di(2-pyridyl)ketone was purchased from Aldrich or from Frontier Chemicals. 1,3,5-tris(2-bromophenyl)benzene¹ was prepared according to literature procedures.



Synthesis of 1, 3, 5-Tris(2-di(2'-pyridyl)hydroxymethylphenyl)benzene (H_3L). In the glovebox, a Schlenk flask equipped with a stir bar was charged with 1,3,5-tris(2-bromophenyl)benzene (4.0 g, 7.37 mmol) and diethyl ether (80 mL). On the Schlenk line, the suspension was cooled to -78°C , and $t\text{-BuLi}$ (1.61 M, 27.9 mL, 44.9 mmol) was added slowly via syringe. The mixture was stirred for 15 min. at -78°C , and a solution of di(2-pyridyl)ketone (4.21 g, 22.8 mmol) in diethyl ether (30 mL) was added slowly via cannula transfer. The reaction mixture was allowed to warm to room temperature and stirred for 8 h under nitrogen. The mixture was quenched with methanol (30 mL), and the orange solution was diluted with water and extracted with dichloromethane. The organic layer was washed with brine and dried over magnesium sulfate, then filtered. The solvent was removed under reduced pressure, and the

yellow residue was recrystallized from acetone/dichloromethane to yield the product as a white solid (2.65 g, 42%). ^1H NMR (300 MHz, CDCl_3 , 25 °C): δ 8.41 (d, $J = 6$ Hz, 6 H, *a*), 7.66 (bs, 6 H, *c*), 7.55 (bs, 6 H, *d*), 7.25 (t, $J = 7.5$ Hz, 3 H, *f*), 7.13 (t, $J = 7.5$ Hz, 3 H, *g*), 7.02 (bs, 6 H, *b*), 6.81 (bs, 3 H, *e*), 6.74 ($J = 6$ Hz, 3 H, *h*), 6.37 (bs, 3 H, OH), 6.14 (bs, 3 H, *j*). ^{13}C NMR (CDCl_3): δ 164.0, 147.2, 144.0, 143.5, 139.5, 136.2, 133.2, 129.2, 126.6, 126.1, 123.7, 121.9, 81.9. IR (CH_2Cl_2): 3330, 1751 cm^{-1} . HRMS (FAB+): calcd. for $\text{C}_{57}\text{H}_{43}\text{N}_6\text{O}_3$: 859.3397; found: 859.3436 [M+H].

Synthesis of $\text{LMn}_3(\text{OAc})_3$. Under an N_2 atmosphere, H_3L (335.5 mg, 0.39 mmol) and $\text{Mn}(\text{OAc})_2$ (202.8 mg, 1.17 mmol) were combined in a scintillation vial equipped with a stirbar, to which a 1:1 $\text{CH}_3\text{CN}/\text{H}_2\text{O}$ solution was added. To the stirring tan suspension was added a 1 M solution of KOH in H_2O . After the solution became yellow and homogeneous, the solvent was removed *in vacuo*. The residue was partially dissolved in CHCl_3 then dried under vacuum twice to ensure evaporation of CH_3CN and H_2O . The residue was triturated in CHCl_3 and a white solid was filtered from the yellow solution. Yellow crystals were grown by vapor diffusion of diethyl ether into a CHCl_3 solution of $\text{LMn}_3(\text{OAc})_3$ (247 mg, 53%). ^1H NMR (300 MHz, CDCl_3 , 25 °C): δ 41.76 ($\Delta\nu_{1/2} = 2000$ Hz), 11.15 ($\Delta\nu_{1/2} = 1230$ Hz), 4.49 ($\Delta\nu_{1/2} = 850$ Hz), -10.56 ($\Delta\nu_{1/2} = 1530$ Hz). UV-Vis (CH_2Cl_2 , $\lambda_{\max} (\varepsilon)$): 256 (47,200 $\text{M}^{-1} \text{cm}^{-1}$); 350 (585 $\text{M}^{-1} \text{cm}^{-1}$) nm. Anal. Calcd. for $\text{C}_{63}\text{H}_{48}\text{Mn}_3\text{N}_6\text{O}_9$: C, 63.17; H, 4.04; N, 7.02. Found: C, 62.96; H, 4.20; N, 6.77.

Synthesis of $\text{LFe}_3(\text{OAc})_3$. In a glovebox, a scintillation vial equipped with a stir bar was charged with a suspension of $\text{Fe}(\text{OAc})_2$ (0.061 g, 0.349 mmol) in CH_2Cl_2 (2 mL). Triethylamine (0.052 mL, 0.407 mmol) was added via syringe, and then a solution of H_3L (0.100 g, 0.116 mmol) in CH_2Cl_2 (3 mL) was added. The pale yellow mixture was stirred at room temperature and slowly darkened over 20 h to form a homogeneous orange solution. The solvent was removed under reduced pressure and the residue was recrystallized twice from CH_2Cl_2 /diethyl ether to yield the product as orange-red crystals (0.087 g, 62%). ^1H NMR (300 MHz, CD_2Cl_2 , 25 °C): δ 109.04 (3 H), 69.06 (3 H), 65.32 (6 H), 43.77 (3 H), 38.34 (9 H), 37.96 (3 H), 28.40 (3 H), 13.43 (3 H), 12.93 (3 H), 9.47 (3 H), 8.08 (3 H), 3.49 (3 H), -4.13 (3 H). UV-Vis (CH_2Cl_2 , $\lambda_{\max} (\varepsilon)$): 254 (50,500 $\text{M}^{-1} \text{cm}^{-1}$); 443 (2610 $\text{M}^{-1} \text{cm}^{-1}$); 793 (83 $\text{M}^{-1} \text{cm}^{-1}$) nm. Anal. Calcd. for $\text{C}_{63}\text{H}_{48}\text{Fe}_3\text{N}_6\text{O}_9$: C, 63.02; H, 4.03; N, 7.00. Found: C, 62.91; H, 3.97; N, 6.90.

Synthesis of $\text{LCo}_3(\text{OAc})_3$. H_3L (310.5 mg, 0.36 mmol) was suspended in a 1:1 solution of CH_3CN and H_2O (~6 mL). $\text{Co}(\text{OAc})_2 \cdot 4\text{H}_2\text{O}$ (270.1 mg, 1.08 mmol) was added as a crystalline solid to the stirring suspension. To this mixture, a 1 M KOH solution in H_2O (1.1 mL) was added dropwise. The reaction was stirred at room temperature until it became a homogenous solution (12 h), then the solvent was removed *in vacuo*. The red-purple solid was extracted with CH_2Cl_2 , and the resulting red solution was dried *in vacuo* for 8 hrs. The resulting red-purple powder was dissolved in CHCl_3 and diethyl ether was allowed to diffuse into the solution slowly as a vapor. White precipitate collected at the bottom of the vial and the red homogeneous solution was decanted off. This precipitation procedure was repeated until no more white precipitate appeared and the red crystalline clusters of $\text{LCo}_3(\text{OAc})_3$ were collected (250 mg, 57%). ^1H NMR (300 MHz, CDCl_3 , 25 °C): δ 128.16 (3 H), 89.12 (3 H), 65.30 (3 H), 57.02 (3 H), 36.52 (3 H), 27.29 (3 H), 16.67 (3 H), 14.72 (9 H), 10.17 (3 H), 8.99 (3 H), 6.06 (3 H), 1.01 (3 H), -0.42 (3 H), -14.24 (3 H). UV-Vis: (CH_2Cl_2 , $\lambda_{\max} (\varepsilon)$): 251 (39,000 $\text{M}^{-1} \text{cm}^{-1}$); 331 (2350 $\text{M}^{-1} \text{cm}^{-1}$); 457 (76 $\text{M}^{-1} \text{cm}^{-1}$); 551 (86 $\text{M}^{-1} \text{cm}^{-1}$); 580 (70 $\text{M}^{-1} \text{cm}^{-1}$) nm. Anal. Calcd. for

$C_{63}H_{48}Co_3N_6O_9$: C, 62.54; H, 4.00; N, 6.95. Found: C, 62.36; H, 4.02; N, 6.90.

Synthesis of $LNi_3(OAc)_3$. H_3L (270.4 mg, 0.31 mmol) was suspended in a 1:1 solution of CH_3CN and H_2O (~5 mL). $Ni(OAc)_2 \cdot 4H_2O$ (235.0 mg, 0.94 mmol) was added as a crystalline solid to the stirring suspension. To this, a 1 M KOH solution in H_2O (0.94 mL) was added dropwise. When all of the H_3L was dissolved to give a green homogeneous solution (~12 h), the solvent was removed under reduced pressure. The green residue was taken up in CH_2Cl_2 and a white solid was filtered from the green solution. The solution was pumped down and dried *in vacuo* for 8 hrs. The resulting green powder was dissolved in $CHCl_3$ and diethyl ether was allowed to diffuse into the solution as a vapor. White precipitate collected at the bottom of the vial and the green homogeneous solution was decanted off. This precipitation procedure was repeated until no more white precipitate appeared and green crystalline clusters of $LNi_3(OAc)_3$ grew (100 mg, 27%). 1H NMR (300 MHz, $CDCl_3$, 25 °C): δ 150.81 (3 H), 136.93 (3 H), 58.87 (3 H), 46.53 (3 H), 34.58 (3 H), 32.08 (3 H), 21.36 (9 H), 15.85 (3 H), 12.31 (6 H), 10.76 (3 H), 7.74 (3 H), 4.90 (3 H), 3.8 (3 H). UV-Vis: (CH_2Cl_2 , λ_{max} (ϵ)): 254 (35,900 $M^{-1} cm^{-1}$); 385 (192 $M^{-1} cm^{-1}$); 450 (45 $M^{-1} cm^{-1}$); 500 (29 $M^{-1} cm^{-1}$); 676 (37 $M^{-1} cm^{-1}$) nm. Anal. Calcd. for $C_{63}H_{48}N_6Ni_3O_9$: C, 62.58; H, 4.00; N, 6.95. Found: C, 62.49; H, 4.20; N, 7.05.

Synthesis of $LCu_3(OAc)_3$. A scintillation vial equipped with a stir bar was charged with H_3L (0.100 g, 0.116 mmol) and $Cu(OAc)_2 \cdot H_2O$ (0.071 g, 0.355 mmol). Dichloromethane (5 mL) was added, and then triethylamine (0.052 mL, 0.407 mmol) was added via syringe. The mixture was stirred at room temperature for 12 h, becoming a homogeneous green mixture. The solvent was removed under reduced pressure and the green residue was washed with THF (5 mL), then recrystallized from CH_2Cl_2 /diethyl ether to yield $LCu_3(OAc)_3$ as clusters of pale green needles (0.041 g, 29%). 1H NMR (500 MHz, $CDCl_3$, 25 °C): δ 126.26 (3 H), 49.44 (3 H), 36.45 (3 H), 33.15 (3 H), 22.02 (3 H), 12.93 (3 H), 10.96 (3 H), 9.80 (9 H), 8.78 (6 H), 8.12 (3 H), 6.55 (3 H), 6.08 (3 H). UV-Vis (CH_2Cl_2 , λ_{max} (ϵ)): 253 (49,100 $M^{-1} cm^{-1}$); 860 (270 $M^{-1} cm^{-1}$) nm. Anal. Calcd. for $C_{63}H_{48}Cu_3N_6O_9$: C, 61.83; H, 3.95; N, 6.87. Anal. Calcd. for $C_{63}H_{50}Cu_3N_6O_{10}$ ($LCu_3(OAc)_3 \cdot H_2O$): C, 60.94; H, 4.06; N, 6.77. Found: C, 60.79; H, 4.04; N, 6.92.

Synthesis of $LZn_3(OAc)_3$. A scintillation vial equipped with a stir bar was charged with H_3L (0.100 g, 0.116 mmol) and $Zn(OAc)_2$ (0.065 g, 0.355 mmol). Dichloromethane (5 mL) was added, then triethylamine (0.052 mL, 0.407 mmol) was added via syringe. The yellow solution was stirred at room temperature for 12 h, and the solvent was removed under reduced pressure. The pale pink residue was washed with THF, then recrystallized twice from CH_2Cl_2 /diethyl ether to yield $LZn_3(OAc)_3$ as colorless crystals (0.024 g, 17%). 1H NMR (500 MHz, $CDCl_3$, 25 °C): δ 8.70 (d, $J = 4.5$ Hz, 3 H, *a*), 8.02 (t, $J = 7.5$ Hz, 3 H, *f*), 7.86 (t, $J = 7.5$ Hz, 3 H, *g*), 7.80 (d, $J = 8$ Hz, 3 H, *d*), 7.74 (d, $J = 4.5$ Hz, 3 H, *a'*), 7.37 (dd, $J = 7.5, 4.5$ Hz, 3 H, *b* or *b'*), 7.25 (dd, $J = 7.5, 4.5$ Hz, 3 H, *b* or *b'*), 7.21 (t, $J = 8$ Hz, 3 H, *c* or *c'*), 7.17 (t, $J = 7.5$ Hz, 3 H, *c* or *c'*), 7.16 (d, $J = 8$ Hz, 3 H, *d'*), 6.98 (d, $J = 7.5$ Hz, 3 H, *e*), 6.51 (d, $J = 7.5$ Hz, 3 H, *h*), 5.66 (s, 3 H, *j*), 1.42 (s, 9 H, OAc). ^{13}C NMR (125.70 MHz, $CDCl_3$, 25 °C): δ 177.5, 165.7, 164.0, 150.6, 147.1, 144.7, 142.5, 141.5, 140.0, 138.7, 131.3, 130.5, 127.7, 127.0, 126.7, 126.2, 123.8, 123.6, 121.6, 84.4, 23.6. UV-Vis (CH_2Cl_2 , λ_{max} (ϵ)): 253 (48,700 $M^{-1} cm^{-1}$) nm. Anal. Calcd. for $C_{63}H_{48}N_6O_9Zn_3$: C, 61.56; H, 3.94; N, 6.84. Anal. Calcd. for $C_{63}H_{50}N_6O_{10}Zn_3$ ($LZn_3(OAc)_3 \cdot H_2O$): C, 60.67; H, 4.04; N, 6.74. Found: C, 60.93; H, 4.09; N, 6.71.

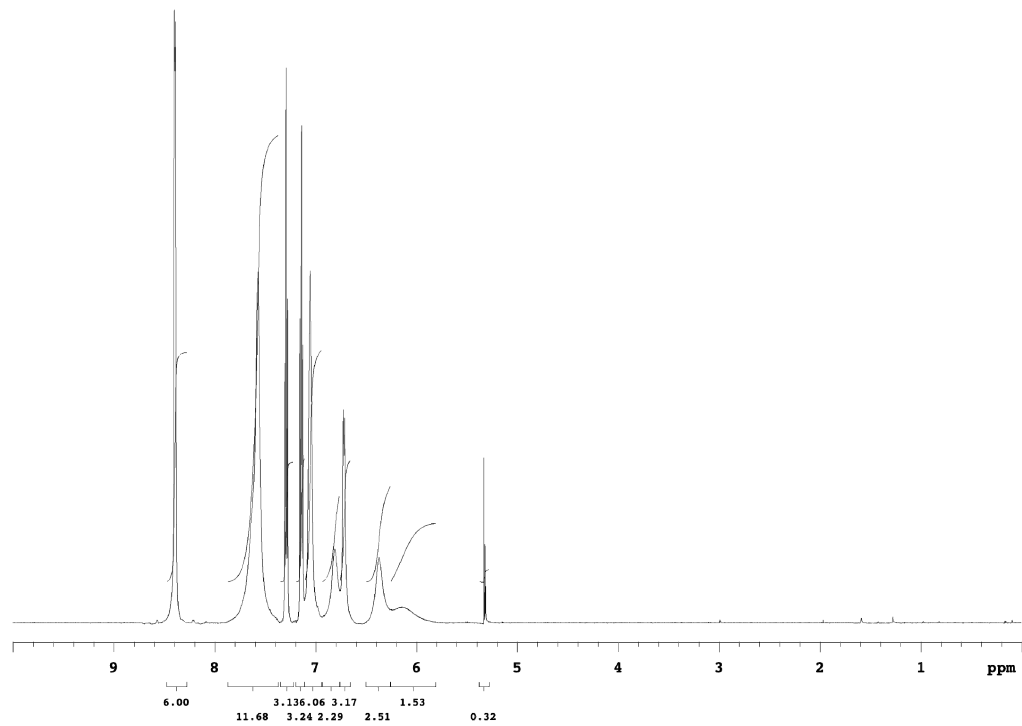


Figure S1. ¹H NMR spectrum of H₃L in CD₂Cl₂ at 25 °C.

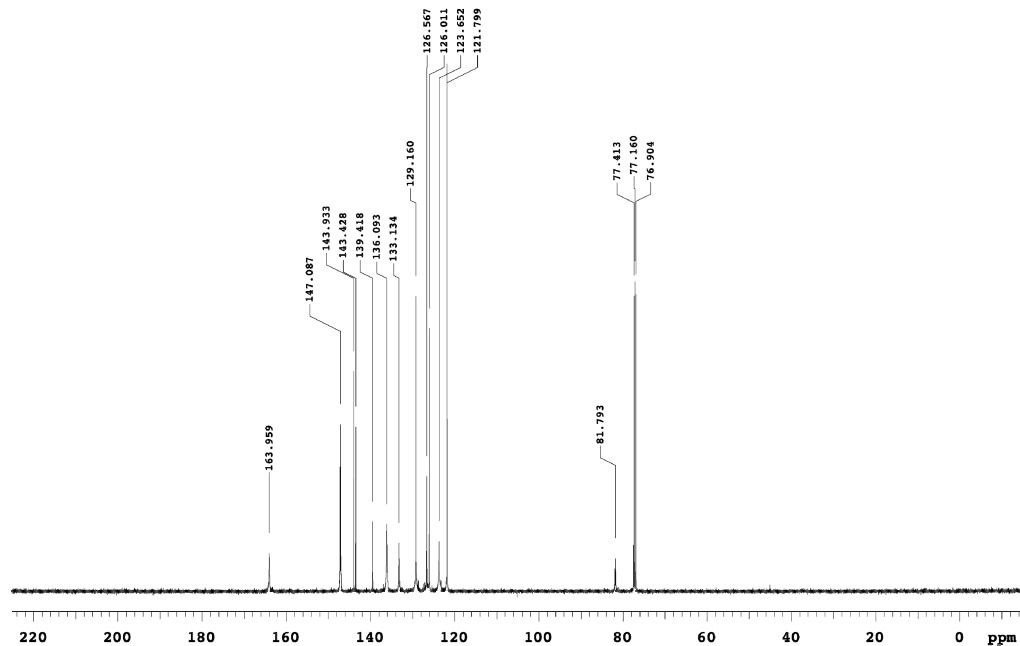


Figure S2. ¹³C NMR spectrum of H₃L in CDCl₃ at 25 °C.

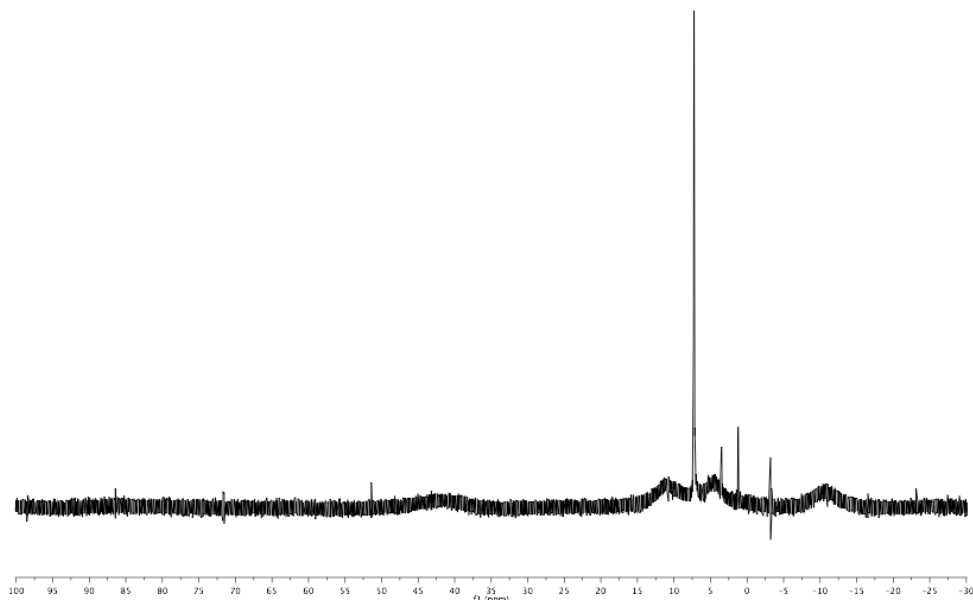


Figure S3. ¹H NMR spectrum of LMn₃(OAc)₃ in CDCl₃ at 25 °C.

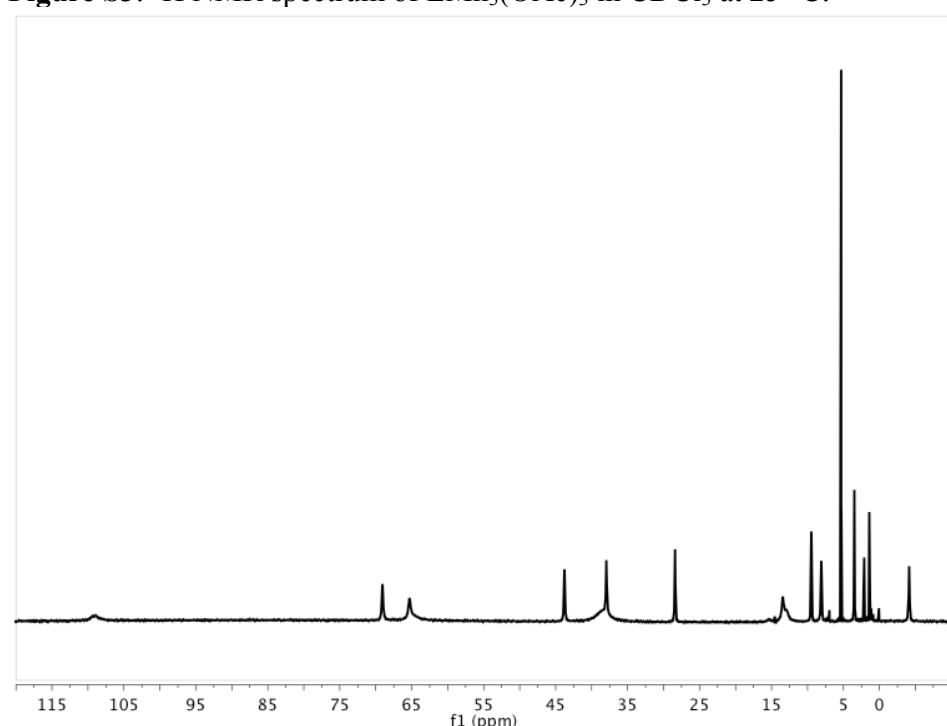


Figure S4. ¹H NMR spectrum of LFe₃(OAc)₃ in CD₂Cl₂ at 25 °C.

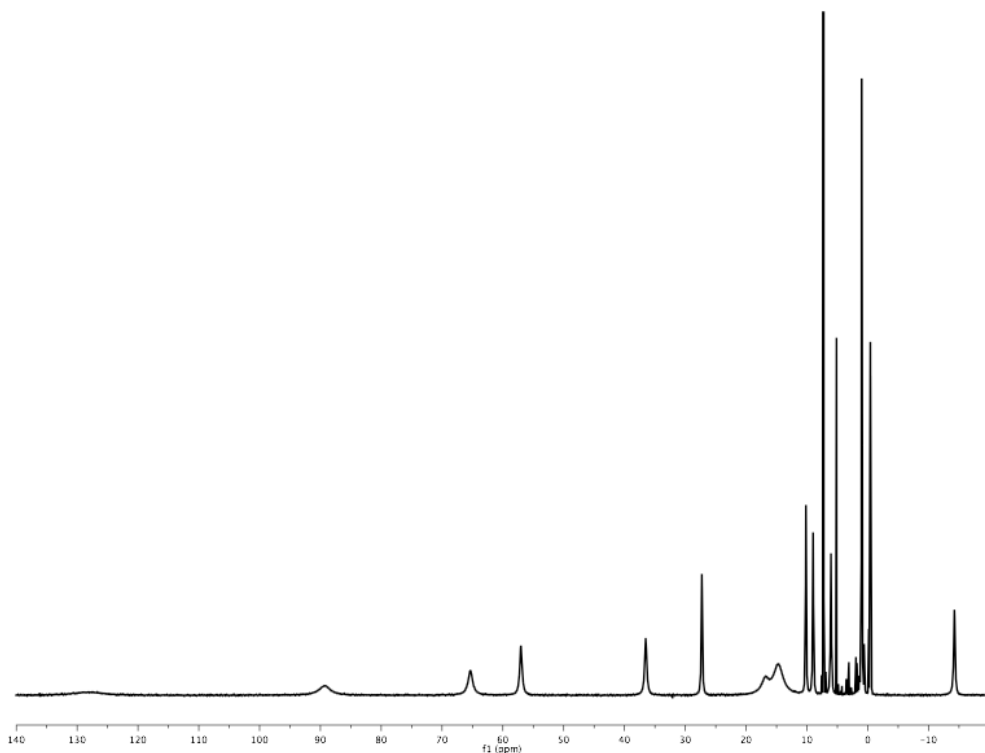


Figure S5. ¹H NMR spectrum of LCo₃(OAc)₃ in CDCl₃ 25 °C.

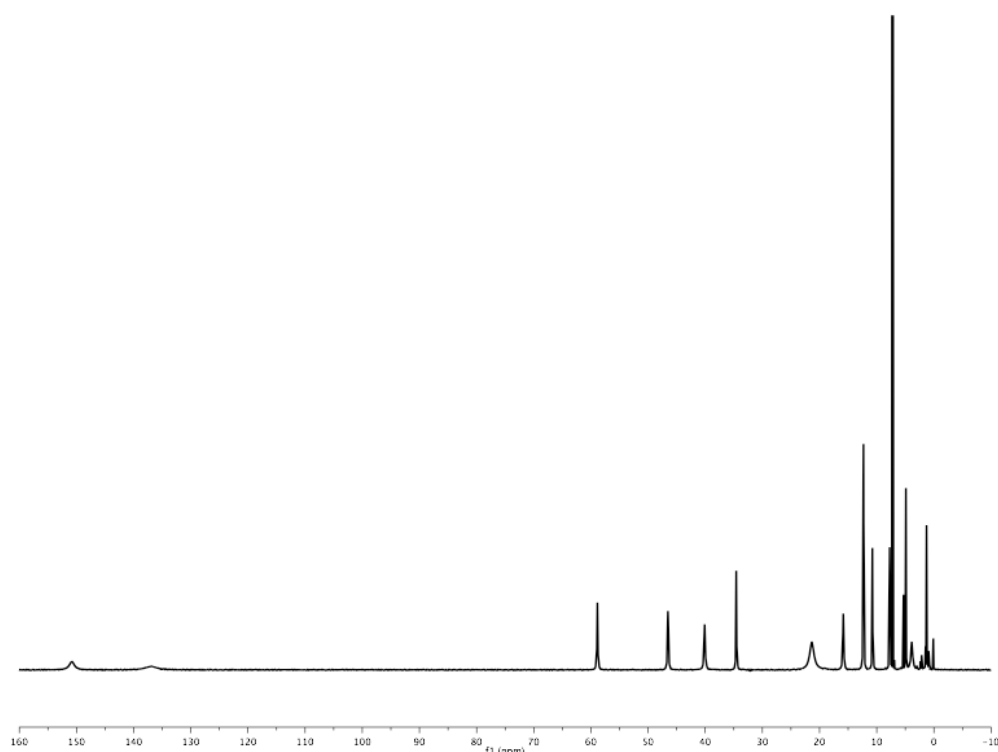


Figure S6. ¹H NMR spectrum of LNi₃(OAc)₃ in CDCl₃ at 25 °C.

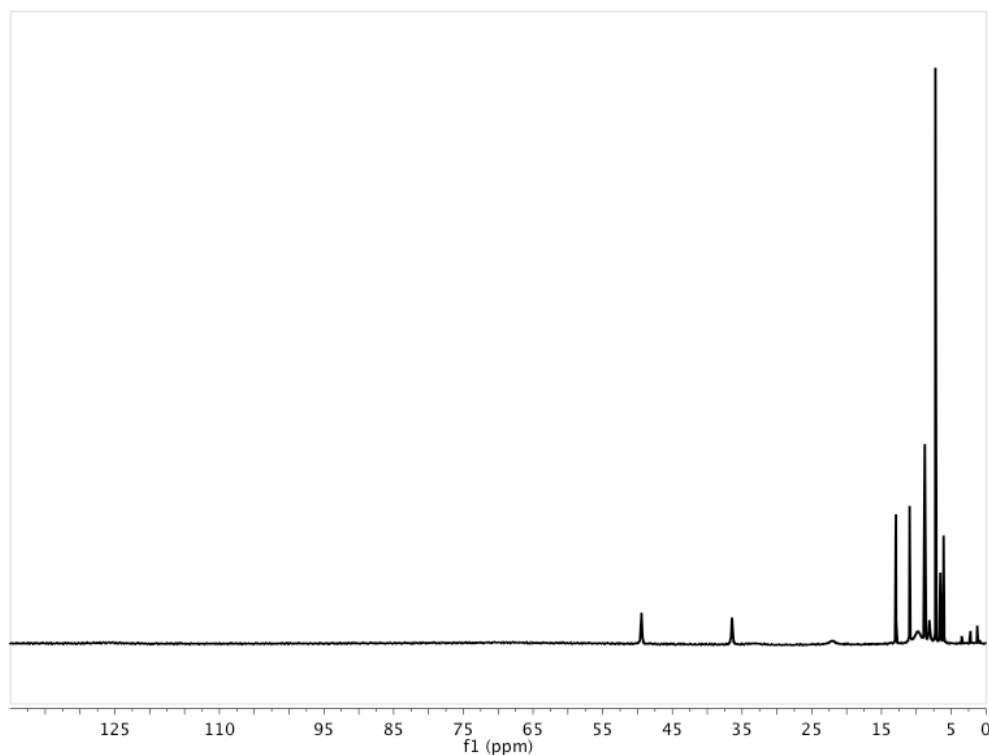


Figure S7. ¹H NMR spectrum of LCu₃(OAc)₃ in CDCl₃ at 25 °C.

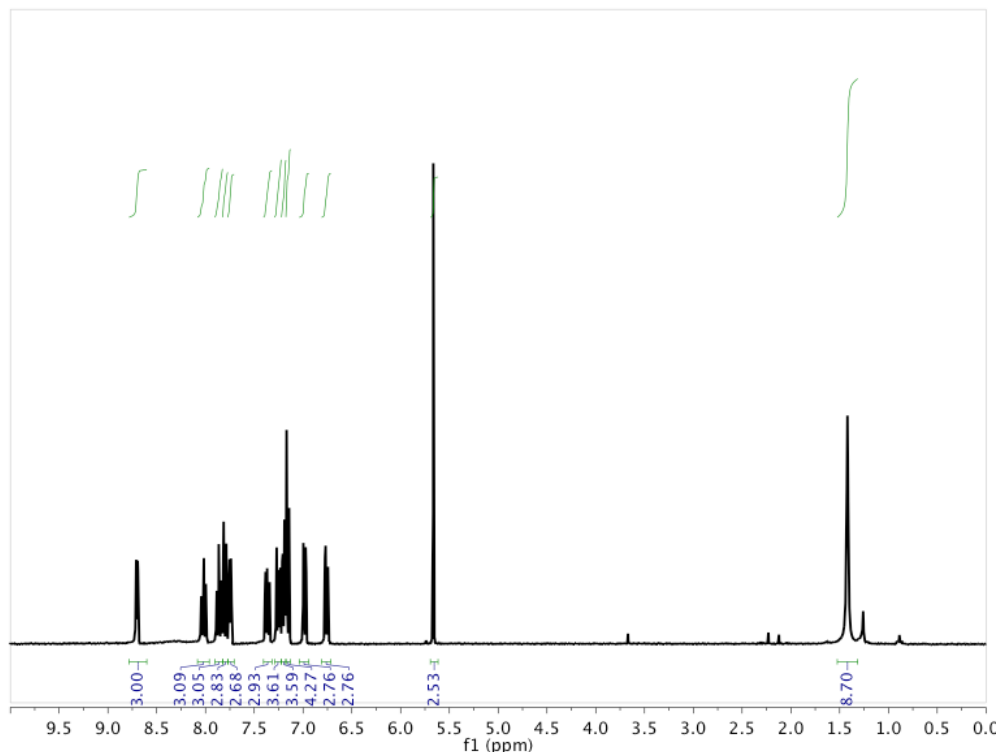


Figure S8. ¹H NMR spectrum of LZn₃(OAc)₃ in CDCl₃ at 25 °C.

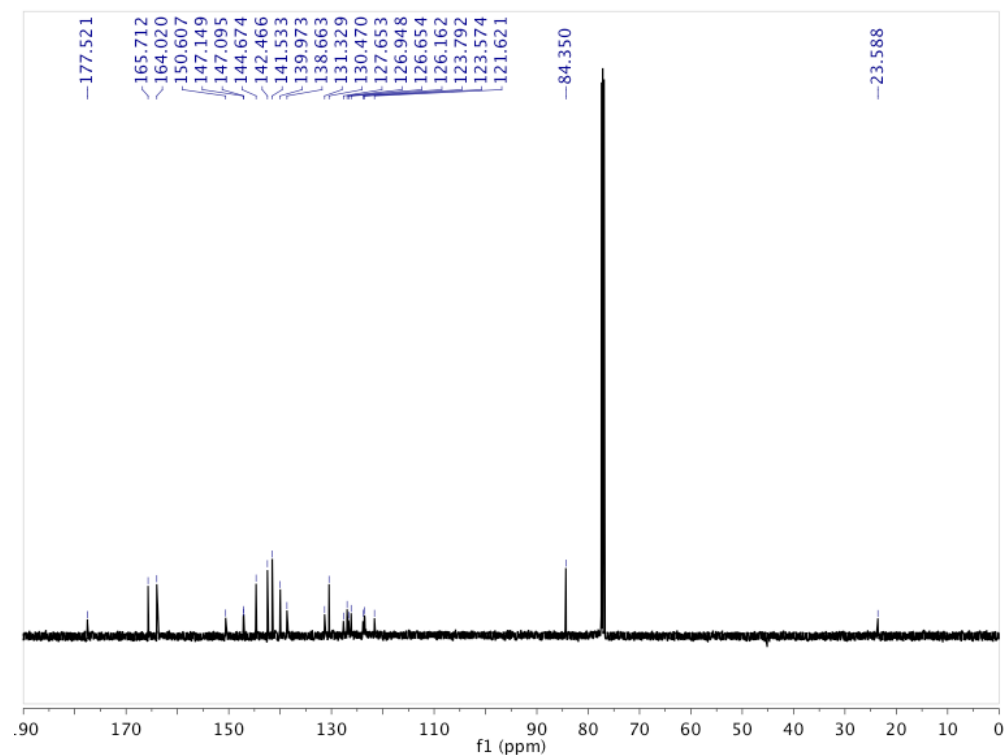


Figure S9. ^{13}C NMR spectrum of $\text{LZn}_3(\text{OAc})_3$ in CDCl_3 at 25°C .

Magnetic Susceptibility Measurements

General Considerations. Magnetic susceptibility measurements were carried out in the Molecular Materials Research Center in the Beckman Institute of the California Institute of Technology on a Quantum Design MPMS instrument running MPMS Multivu software. Crystalline samples (0.030–0.100 g) were powdered and suspended in clear plastic straws in gelatin capsules. Data were recorded at 0.5 and 5 T from 4–300 K. Diamagnetic corrections were made using Pascal's constants as follows: −710, −648, −645, −645, and $-642 \times 10^{-6} \text{ cm}^3/\text{mol}$ respectively for M = Mn, Fe, Co, Ni, and Cu. The data for $\text{LMn}_3(\text{OAc})_3$ were processed and simulated with the inclusion of one equivalent of chloroform, which was found to be in the sample by both elemental analysis and ^1H NMR spectroscopy. Anal. Calcd. for $\text{C}_{64}\text{H}_{39}\text{Cl}_3\text{Mn}_3\text{N}_6\text{O}_9$ ($\text{LMn}_3(\text{OAc})_3 \bullet \text{CHCl}_3$): C, 58.35; H, 3.75; N, 6.38. Found: C, 58.74; H, 3.87; N, 6.31.

The $\chi_M T$ data were fit to the magnetic susceptibility equation derived from the isotropic spin Hamiltonian for two coupling constants, J and J_{13} [Eq. (1)].

$$\hat{H} = -2J[\hat{S}_1\hat{S}_2 + (\hat{S}_2\hat{S}_3)] - 2J_{13}[\hat{S}_3\hat{S}_1] \quad (1)$$

The Kambe vector method² yields the magnetic susceptibility equation [Eq. (2)]. In this equation, spin levels are defined by the quantum number $S' = 3S, 3S-1, 3S-2, \dots, 0$ or $\frac{1}{2}$, where $S = 5/2, 2, 3/2, 1$, and $1/2$ respectively for M = Mn, Fe, Co, Ni, and Cu. Application of the Van Vleck equation gives the energy of each spin state [Eq. (3)].³ The multiplicity of each spin level is defined by $\Omega(S')$.

$$\chi_M = \frac{N_A \beta^2 g^2}{3kT} \frac{\sum S'(S'+1)(2S'+1)\Omega(S') \exp(-W(S')/kT)}{\sum (2S'+1)\Omega(S') \exp(-W(S')/kT)} \quad (2)$$

$$W(S') = -J[S'(S'+1) - 3S(S+1)] \quad (3)$$

The data were fit using Matlab by minimizing $R = \sum |(\chi_M T)_{obs} - (\chi_M T)_{calcd}|^2 / \sum (\chi_M T)_{obs}^2$.

The $\chi_M T$ data below $T = 40$ K for $\text{LCu}_3(\text{OAc})_3$ did not fit the model equation as well as the higher temperature data. This discrepancy may be due to other exchange interactions whose effects are stronger at low temperatures, such as intermolecular interactions or interactions due to temperature-dependent structural changes.

Crystallographic Information:

Crystallographic data have been deposited at the CCDC, 12 Union Road, Cambridge CB2 1EZ, UK and copies can be obtained on request, free of charge, by quoting the publication citation and the deposition numbers 787163 (Mn), 803594 (Fe), 777599 (Co), 803595 (Ni), 803593 (Cu), and 803592 (Zn).

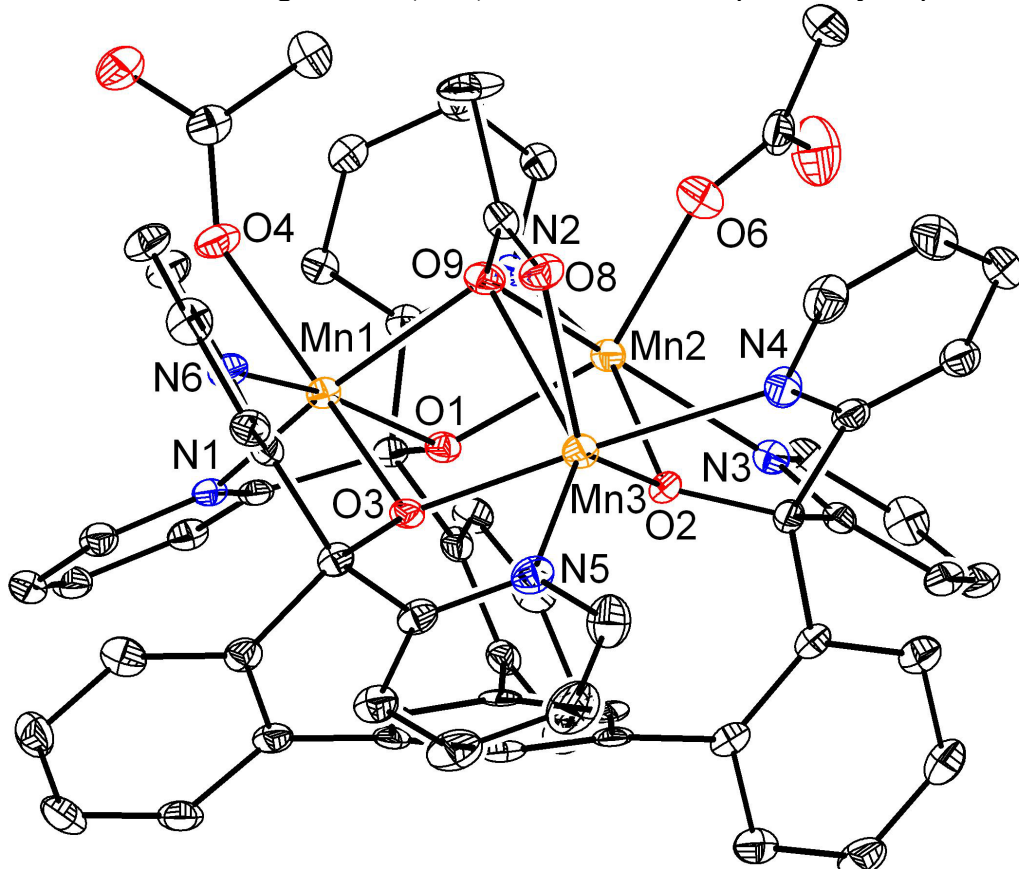
Table S1. Crystal and refinement data for $\text{LM}_3(\text{OAc})_3$ (M = Mn, Fe, Co, Ni, Cu, Zn).

	$\text{LMn}_3(\text{OAc})_3$	$\text{LFe}_3(\text{OAc})_3$	$\text{LCo}_3(\text{OAc})_3$	$\text{LNi}_3(\text{OAc})_3$	$\text{LCu}_3(\text{OAc})_3$	C
empirical formula	$\text{C}_{63}\text{H}_{48}\text{Mn}_3\text{N}_6\text{O}_9$	$\text{C}_{63}\text{H}_{48}\text{Fe}_3\text{N}_6\text{O}_9$	$\text{C}_{63}\text{H}_{48}\text{Co}_3\text{N}_6\text{O}_9$	$\text{C}_{63}\text{H}_{48}\text{Ni}_3\text{N}_6\text{O}_9$	$\text{C}_{63}\text{H}_{48}\text{Cu}_3\text{N}_6\text{O}_9$	C
formula wt	1197.90	1200.62	1209.89	1209.17	1164.65	
T (K)	100(2)	100(2)	100(2)	100(2)	100(2)	
a, Å	10.5708(8)	10.6327(4)	20.8675(10)	20.7019(9)	18.9118(5)	
b, Å	19.6592(14)	18.9722(8)	20.8675(10)	20.7019(9)	19.0501(5)	
c, Å	20.2109(15)	19.6009(8)	10.5670(6)	10.6229(6)	36.0732(9)	
α , deg	71.889(4)	72.453(2)	90	90	90	

β , deg	88.967(4)	89.924(2)	90	90	90
γ , deg	75.160(4)	75.857(2)	120	120	90
V , \AA^3	3850.2(5)	3644.5(3)	3985.0(4)	3942.7(3)	12996.1(6)
Z	2	2	3	3	8
cryst syst	triclinic	triclinic	trigonal	trigonal	orthorhombic
space group	P-1	P-1	R 3	R 3	P bcn
d_{calcd} , g/ cm^3	1410	1094	1512	1528	1190
θ range, deg	2.00–30.2	1.98–30.60	2.23–30.10	1.97–30.16	1.89–26.40
μ , mm^{-1}	0.531	0.638	0.993	1.132	1.023
abs cor	none	none	Semi-empirical from equivalents	none	none
GOF	2.775	3.896	2.172	2.887	2.988
		0.0576, 0.0576,			
R1, ^a wR2 ^b ($I > 2\sigma(I)$)	0.0504, 0.0863	0.1052	0.0380, 0.0788	0.0443, 0.0690	0.0481, 0.0898

^a $R1 = \frac{\sum ||F_o|| - |F_c||}{\sum |F_o||}$. ^b $wR2 = \left\{ \frac{\sum [w(F_o^2 - F_c^2)^2]}{\sum [w(F_o^2)^2]} \right\}^{1/2}$.

Figure S10. Structural drawing of $\text{LMn}_3(\text{OAc})_3$ with 50% thermal probability ellipsoids.



Special refinement details for $\text{LMn}_3(\text{OAc})_3$. Crystals were mounted in a loop with oil then placed on the diffractometer under a nitrogen stream at 100K. The solvent contains four molecules of chloroform and one of diethyl ether. Although they were discernable we were unable to obtain a satisfactory solvent model due to disorder. Due to the considerable percentage of the unit cell occupied by the solvent (37.4%) and the presence of strong scatterers (12 Cl atoms) SQUEEZE⁴ was employed to produce a bulk solvent correction to the observed

intensities. The program accounted for 430 electrons of approximately 550 expected. The resulting model is vastly superior to the model including solvent specifically. Refinement of F^2 against ALL reflections. The weighted R-factor (wR) and goodness of fit (S) are based on F^2 , conventional R-factors (R) are based on F, with F set to zero for negative F^2 . The threshold expression of $F^2 > 2s(F^2)$ is used only for calculating R-factors(gt) etc. and is not relevant to the choice of reflections for refinement. R-factors based on F^2 are statistically about twice as large as those based on F, and R-factors based on ALL data will be even larger. All esds (except the esd in the dihedral angle between two l.s. planes) are estimated using the full covariance matrix. The cell esds are taken into account individually in the estimation of esds in distances, angles and torsion angles; correlations between esds in cell parameters are only used when they are defined by crystal symmetry. An approximate (isotropic) treatment of cell esds is used for estimating esds involving l.s. planes.

Table S2. Atomic coordinates ($\times 10^4$) and equivalent isotropic displacement parameters ($\text{\AA}^2 \times 10^3$) for $\text{LMn}_3(\text{OAc})_3$. $U(\text{eq})$ is defined as the trace of the orthogonalized U^{ij} tensor.

	x	y	z	U_{eq}
Mn(1)	7930(1)	1884(1)	5911(1)	13(1)
Mn(2)	8658(1)	592(1)	7529(1)	15(1)
Mn(3)	7434(1)	2417(1)	7390(1)	16(1)
O(1)	7542(1)	892(1)	6592(1)	13(1)
O(2)	7215(2)	1386(1)	7872(1)	14(1)
O(3)	6636(1)	2574(1)	6402(1)	13(1)
O(4)	9488(2)	1620(1)	5288(1)	21(1)
O(5)	11223(2)	1857(1)	4718(1)	29(1)
O(6)	10393(2)	551(1)	8042(1)	27(1)
O(7)	11088(2)	-626(1)	8693(1)	41(1)
O(8)	9270(2)	2686(1)	7153(1)	20(1)
O(9)	9268(2)	1707(1)	6821(1)	17(1)
N(1)	6842(2)	1456(1)	5264(1)	14(1)
N(2)	9582(2)	-268(1)	6967(1)	15(1)
N(3)	7759(2)	-40(1)	8467(1)	16(1)
N(4)	8287(2)	2066(1)	8542(1)	19(1)
N(5)	5975(2)	3503(1)	7133(1)	19(1)
N(6)	7972(2)	3120(1)	5368(1)	16(1)
C(1)	4609(2)	1478(1)	6322(1)	15(1)
C(2)	4933(2)	882(1)	6941(1)	15(1)
C(3)	4843(2)	1028(1)	7571(1)	16(1)
C(4)	4506(2)	1754(1)	7595(1)	16(1)
C(5)	4215(2)	2335(1)	6976(1)	16(1)
C(6)	4297(2)	2206(1)	6331(1)	16(1)
C(7)	4147(2)	2811(1)	5655(1)	17(1)
C(8)	3260(2)	2837(1)	5132(1)	21(1)
C(9)	3136(2)	3336(2)	4467(1)	24(1)
C(10)	3914(2)	3829(1)	4296(1)	23(1)
C(11)	4799(2)	3807(1)	4800(1)	20(1)
C(12)	4953(2)	3315(1)	5481(1)	16(1)
C(13)	5443(2)	101(1)	6953(1)	16(1)
C(14)	4742(3)	-406(2)	7307(1)	23(1)
C(15)	5172(3)	-1152(2)	7385(1)	24(1)

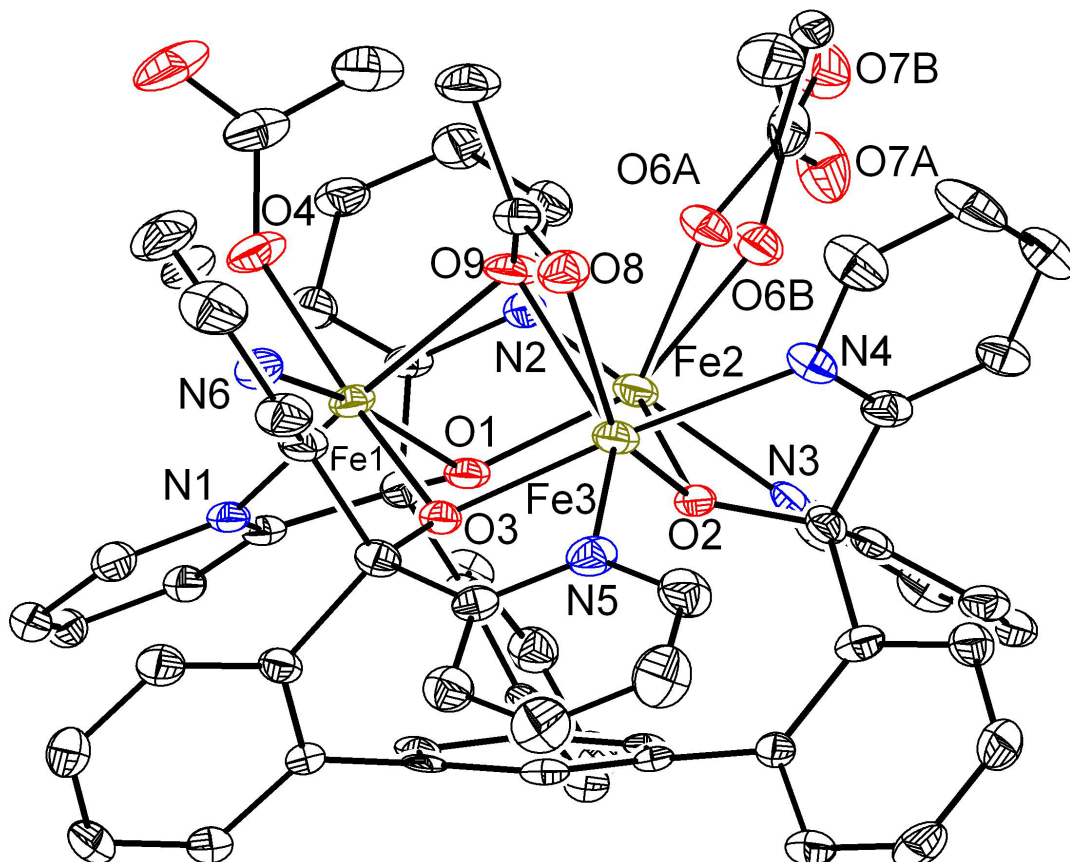
C(16)	6332(2)	-1417(1)	7115(1)	21(1)
C(17)	7033(2)	-924(1)	6758(1)	19(1)
C(18)	6636(2)	-170(1)	6674(1)	14(1)
C(19)	4543(2)	1905(1)	8268(1)	17(1)
C(20)	3389(2)	2350(1)	8427(1)	23(1)
C(21)	3325(3)	2544(1)	9035(1)	24(1)
C(22)	4412(3)	2292(1)	9500(1)	24(1)
C(23)	5572(2)	1848(1)	9346(1)	20(1)
C(24)	5663(2)	1654(1)	8731(1)	14(1)
C(25)	6025(2)	3294(1)	6002(1)	14(1)
C(26)	7511(2)	348(1)	6289(1)	13(1)
C(27)	7015(2)	1196(1)	8581(1)	15(1)
C(28)	7110(2)	3619(1)	5601(1)	14(1)
C(29)	7253(2)	4313(1)	5507(1)	18(1)
C(30)	8313(2)	4524(1)	5153(1)	22(1)
C(31)	9172(2)	4023(1)	4902(1)	23(1)
C(32)	8978(2)	3328(1)	5021(1)	21(1)
C(33)	5427(2)	3760(1)	6478(1)	16(1)
C(34)	4410(2)	4403(1)	6252(1)	21(1)
C(35)	3935(3)	4802(2)	6706(2)	28(1)
C(36)	4495(3)	4535(2)	7381(2)	33(1)
C(37)	5499(3)	3885(2)	7575(1)	28(1)
C(38)	6948(2)	722(1)	5525(1)	13(1)
C(39)	6496(2)	352(1)	5137(1)	17(1)
C(40)	5870(2)	753(1)	4479(1)	19(1)
C(41)	5709(2)	1514(1)	4235(1)	19(1)
C(42)	6226(2)	1839(1)	4637(1)	16(1)
C(43)	8945(2)	-149(1)	6356(1)	14(1)
C(44)	9513(2)	-464(1)	5867(1)	15(1)
C(45)	10769(2)	-942(1)	6015(1)	18(1)
C(46)	11411(2)	-1072(1)	6652(1)	21(1)
C(47)	10793(2)	-716(1)	7106(1)	18(1)
C(48)	7119(2)	364(1)	8865(1)	14(1)
C(49)	6583(2)	31(1)	9466(1)	19(1)
C(50)	6672(2)	-725(1)	9660(1)	22(1)
C(51)	7291(3)	-1125(2)	9240(1)	24(1)
C(52)	7833(2)	-766(1)	8654(1)	21(1)
C(53)	8109(2)	1405(1)	8928(1)	18(1)
C(54)	8833(2)	978(1)	9544(1)	20(1)
C(55)	9784(2)	1236(2)	9783(1)	25(1)
C(56)	9989(3)	1904(2)	9392(1)	27(1)
C(57)	9221(3)	2299(2)	8781(1)	25(1)
C(58)	10721(3)	1495(1)	5231(1)	20(1)
C(59)	11597(2)	864(1)	5797(1)	23(1)
C(60)	11192(3)	12(2)	8483(1)	21(1)
C(61)	12330(3)	212(2)	8743(1)	38(1)
C(62)	9843(2)	2172(2)	6915(1)	20(1)
C(63)	11241(2)	2116(2)	6725(2)	34(1)

Table S3. Anisotropic displacement parameters ($\text{\AA}^2 \times 10^4$) for $\text{LMn}_3(\text{OAc})_3$. The anisotropic displacement factor exponent takes the form: $-2\pi^2 [h^2 a^{*2} U^{11} + \dots + 2 h k a^{*} b^{*} U^{12}]$

	U ¹¹	U ²²	U ³³	U ²³	U ¹³	U ¹²
Mn(1)	121(2)	137(2)	144(2)	-49(2)	19(2)	-41(2)
Mn(2)	124(2)	180(2)	146(2)	-64(2)	10(2)	-32(2)
Mn(3)	148(2)	167(2)	158(2)	-43(2)	14(2)	-52(2)
O(1)	114(9)	147(9)	156(9)	-64(7)	7(7)	-43(7)
O(2)	126(9)	175(10)	126(9)	-49(8)	35(7)	-49(8)
O(3)	98(9)	117(9)	150(9)	-21(7)	3(7)	3(7)
O(4)	151(10)	275(11)	251(10)	-142(9)	76(8)	-74(9)
O(5)	250(11)	341(12)	279(11)	-46(10)	73(9)	-131(10)
O(6)	213(11)	333(12)	266(11)	-82(10)	-33(9)	-70(10)
O(7)	591(16)	298(13)	304(12)	-33(10)	-26(11)	-131(12)
O(8)	167(10)	232(11)	245(10)	-126(9)	54(8)	-60(8)
O(9)	130(9)	182(10)	206(10)	-61(8)	0(7)	-70(8)
N(1)	89(11)	164(12)	150(11)	-36(9)	19(9)	-24(9)
N(2)	111(11)	168(12)	176(11)	-56(9)	-8(9)	-19(9)
N(3)	142(12)	170(12)	162(11)	-50(9)	0(9)	-30(10)
N(4)	212(13)	220(13)	172(11)	-73(10)	23(9)	-110(10)
N(5)	178(12)	186(12)	223(12)	-101(10)	45(10)	-42(10)
N(6)	144(12)	157(12)	193(11)	-59(9)	38(9)	-59(10)
C(1)	54(13)	237(15)	182(13)	-77(12)	25(10)	-56(11)
C(2)	39(12)	192(14)	234(14)	-65(12)	17(10)	-60(11)
C(3)	70(13)	222(15)	191(13)	-36(11)	37(10)	-85(11)
C(4)	52(13)	232(15)	213(14)	-88(12)	33(10)	-58(11)
C(5)	62(13)	191(14)	249(14)	-101(12)	43(11)	-43(11)
C(6)	64(13)	220(15)	177(13)	-10(11)	-6(10)	-60(11)
C(7)	105(13)	178(14)	202(14)	-70(11)	30(11)	-6(11)
C(8)	109(14)	249(16)	263(15)	-58(13)	18(11)	-53(12)
C(9)	165(15)	283(17)	260(15)	-90(13)	-75(12)	-11(13)
C(10)	242(16)	201(15)	183(14)	-4(12)	-37(12)	-27(13)
C(11)	186(15)	126(14)	262(15)	-54(12)	-14(12)	-19(12)
C(12)	139(14)	142(14)	180(13)	-65(11)	29(11)	-5(11)
C(13)	150(14)	185(14)	152(13)	-38(11)	-19(11)	-68(12)
C(14)	227(16)	256(16)	241(15)	-81(13)	45(12)	-125(13)
C(15)	255(16)	253(16)	239(15)	-41(13)	48(12)	-164(14)
C(16)	239(16)	140(14)	248(15)	-44(12)	-16(12)	-70(12)
C(17)	163(14)	196(15)	205(14)	-66(12)	-7(11)	-53(12)
C(18)	155(14)	163(14)	128(12)	-41(11)	-7(10)	-84(11)
C(19)	150(14)	183(14)	192(14)	-68(11)	68(11)	-57(12)
C(20)	153(15)	262(16)	248(15)	-64(13)	23(12)	-34(12)
C(21)	191(15)	231(16)	290(16)	-102(13)	96(13)	-14(13)
C(22)	268(17)	254(16)	208(15)	-101(13)	96(13)	-71(13)
C(23)	181(15)	204(15)	221(14)	-61(12)	54(12)	-71(12)
C(24)	153(14)	127(13)	156(13)	-50(11)	56(11)	-42(11)
C(25)	145(14)	114(13)	159(13)	-39(11)	27(10)	-47(11)
C(26)	112(13)	130(13)	149(12)	-46(11)	16(10)	-40(11)
C(27)	140(14)	206(14)	117(12)	-57(11)	21(10)	-72(11)
C(28)	130(13)	165(14)	139(12)	-40(11)	-12(10)	-43(11)
C(29)	156(14)	166(14)	198(14)	-53(12)	7(11)	-8(12)
C(30)	275(16)	138(14)	264(15)	-53(12)	15(12)	-89(13)
C(31)	191(15)	241(16)	255(15)	-61(13)	93(12)	-98(13)
C(32)	178(15)	193(15)	238(15)	-54(12)	66(12)	-33(12)
C(33)	161(14)	136(14)	200(14)	-44(11)	49(11)	-61(11)

C(34)	175(15)	178(15)	245(15)	-50(12)	37(12)	-39(12)
C(35)	212(16)	209(16)	384(18)	-103(14)	83(14)	7(13)
C(36)	349(19)	316(18)	349(18)	-204(15)	108(15)	-26(15)
C(37)	349(18)	274(17)	237(15)	-108(13)	29(13)	-78(14)
C(38)	81(13)	176(14)	156(13)	-64(11)	25(10)	-43(11)
C(39)	128(14)	191(14)	205(14)	-70(12)	42(11)	-66(12)
C(40)	131(14)	260(16)	213(14)	-95(12)	21(11)	-74(12)
C(41)	128(14)	217(15)	178(14)	-36(12)	-8(11)	-13(12)
C(42)	137(14)	159(14)	183(13)	-44(11)	22(11)	-26(11)
C(43)	158(14)	111(13)	172(13)	-35(11)	22(11)	-76(11)
C(44)	156(14)	138(13)	171(13)	-61(11)	4(11)	-40(11)
C(45)	185(15)	193(14)	190(14)	-74(12)	48(11)	-65(12)
C(46)	177(15)	179(15)	250(15)	-44(12)	6(12)	-13(12)
C(47)	167(14)	198(15)	158(13)	-50(11)	0(11)	-32(12)
C(48)	114(13)	185(14)	139(13)	-60(11)	-14(10)	-32(11)
C(49)	146(14)	215(15)	194(14)	-59(12)	40(11)	-54(12)
C(50)	155(15)	256(16)	222(14)	-17(12)	49(11)	-76(13)
C(51)	292(17)	176(15)	253(15)	-64(12)	-10(13)	-79(13)
C(52)	223(15)	173(15)	230(15)	-60(12)	-10(12)	-39(12)
C(53)	135(14)	255(16)	179(14)	-113(12)	49(11)	-57(12)
C(54)	174(15)	202(15)	202(14)	-60(12)	31(11)	-42(12)
C(55)	212(16)	331(17)	198(14)	-68(13)	-29(12)	-70(14)
C(56)	263(17)	339(18)	274(16)	-112(14)	-16(13)	-170(14)
C(57)	307(17)	259(16)	248(15)	-83(13)	66(13)	-164(14)
C(58)	201(16)	203(15)	247(15)	-135(12)	46(12)	-76(13)
C(59)	265(16)	196(15)	237(15)	-65(12)	-17(12)	-53(13)
C(60)	256(17)	240(16)	121(13)	-59(12)	33(12)	-39(13)
C(61)	213(17)	680(20)	254(16)	-160(17)	-32(13)	-121(17)
C(62)	167(15)	275(16)	157(13)	-53(12)	-20(11)	-54(13)
C(63)	119(15)	470(20)	560(20)	-310(18)	110(14)	-129(14)

Figure S11. Structural drawing of LFe₃(OAc)₃ with 50% thermal probability ellipsoids. One acetate is disordered over two populations, denoted A and B.



Special refinement details for LFe₃(OAc)₃. Crystals were mounted on a glass fiber using Paratone oil then placed on the diffractometer under a nitrogen stream at 100K. Approximately 35% of the unit cell volume is solvent and poorly ordered. To account for solvent the program SQUEEZE⁴ was employed to apply bulk solvent flattening. A total of 685 electrons were accounted for. One of the bound acetate is disordered and was modeled without restraints. Refinement of F² against ALL reflections. The weighted R-factor (wR) and goodness of fit (S) are based on F², conventional R-factors (R) are based on F, with F set to zero for negative F². The threshold expression of F² > 2σ(F²) is used only for calculating R-factors(gt) etc. and is not relevant to the choice of reflections for refinement. R-factors based on F² are statistically about twice as large as those based on F, and R-factors based on ALL data will be even larger. All esds (except the esd in the dihedral angle between two l.s. planes) are estimated using the full covariance matrix. The cell esds are taken into account individually in the estimation of esds in distances, angles and torsion angles; correlations between esds in cell parameters are only used when they are defined by crystal symmetry. An approximate (isotropic) treatment of cell esds is used for estimating esds involving l.s. planes.

Table S4. Atomic coordinates ($\times 10^4$) and equivalent isotropic displacement parameters ($\text{\AA}^2 \times 10^3$) for LFe₃(OAc)₃. U(eq) is defined as the trace of the orthogonalized U^{ij} tensor.

x	y	z	U _{eq}	Occ
---	---	---	-----------------	-----

Fe(1)	3088(1)	6800(1)	970(1)	20(1)	1
Fe(2)	3569(1)	5413(1)	2628(1)	22(1)	1
Fe(3)	2704(1)	7294(1)	2416(1)	21(1)	1
O(1)	2601(2)	5818(1)	1663(1)	20(1)	1
O(2)	2292(2)	6321(1)	2910(1)	19(1)	1
O(3)	1805(2)	7468(1)	1424(1)	17(1)	1
O(4)	4627(2)	6432(1)	459(1)	33(1)	1
O(5)	6418(2)	6680(1)	-26(1)	48(1)	1
O(8)	4226(2)	7889(1)	2094(1)	28(1)	1
O(9)	4461(2)	6793(1)	1868(1)	29(1)	1
O(6A)	5226(5)	5492(4)	3019(4)	25(2)	0.403(9)
O(7A)	6096(9)	4295(4)	3740(3)	40(3)	0.403(9)
O(6B)	5154(4)	5055(4)	3331(3)	36(2)	0.597(9)
O(7B)	7092(5)	4278(3)	3722(2)	45(2)	0.597(9)
N(1)	1959(2)	6428(1)	299(1)	21(1)	1
N(2)	4515(2)	4595(1)	2053(1)	21(1)	1
N(3)	2608(2)	4877(1)	3526(1)	22(1)	1
N(4)	3579(2)	6954(1)	3529(1)	23(1)	1
N(5)	1278(2)	8370(1)	2221(1)	25(1)	1
N(6)	3132(2)	8011(2)	385(1)	27(1)	1
C(1)	-310(2)	6421(2)	1350(2)	20(1)	1
C(2)	-14(2)	5811(2)	2000(2)	16(1)	1
C(3)	-102(2)	5982(2)	2639(2)	19(1)	1
C(4)	-398(2)	6739(2)	2650(2)	18(1)	1
C(5)	-682(2)	7320(2)	2010(2)	20(1)	1
C(6)	-601(2)	7163(2)	1348(2)	18(1)	1
C(7)	498(2)	5010(2)	2020(1)	19(1)	1
C(8)	-185(3)	4474(2)	2397(2)	27(1)	1
C(9)	246(3)	3702(2)	2476(2)	26(1)	1
C(10)	1341(3)	3450(2)	2158(2)	27(1)	1
C(11)	2023(3)	3957(2)	1775(2)	23(1)	1
C(12)	1642(2)	4740(2)	1713(2)	18(1)	1
C(13)	-309(2)	6933(2)	3319(1)	18(1)	1
C(14)	-1387(2)	7434(2)	3486(2)	24(1)	1
C(15)	-1370(3)	7668(2)	4082(2)	30(1)	1
C(16)	-288(3)	7419(2)	4544(2)	29(1)	1
C(17)	815(3)	6895(2)	4415(2)	24(1)	1
C(18)	840(2)	6658(2)	3807(2)	23(1)	1
C(19)	-720(2)	7777(2)	651(2)	19(1)	1
C(20)	-1621(2)	7805(2)	115(2)	23(1)	1
C(21)	-1734(3)	8329(2)	-572(2)	28(1)	1
C(22)	-949(3)	8837(2)	-728(2)	32(1)	1
C(23)	-40(3)	8802(2)	-210(2)	25(1)	1
C(24)	99(2)	8288(2)	485(2)	19(1)	1
C(25)	2532(2)	5273(2)	1323(2)	17(1)	1
C(26)	1991(2)	5680(2)	538(2)	17(1)	1
C(27)	1505(2)	5331(2)	114(2)	21(1)	1
C(28)	933(2)	5762(2)	-570(2)	24(1)	1
C(29)	824(3)	6532(2)	-809(2)	25(1)	1
C(30)	1389(2)	6849(2)	-363(2)	22(1)	1
C(31)	3925(2)	4758(2)	1399(2)	19(1)	1
C(32)	4501(3)	4447(2)	883(2)	26(1)	1
C(33)	5727(3)	3925(2)	1075(2)	30(1)	1

C(34)	6311(3)	3747(2)	1735(2)	32(1)	1
C(35)	5692(3)	4098(2)	2220(2)	30(1)	1
C(36)	2126(2)	6149(2)	3648(2)	21(1)	1
C(37)	2133(2)	5301(2)	3949(2)	20(1)	1
C(38)	1627(2)	4983(2)	4591(2)	24(1)	1
C(39)	1550(3)	4238(2)	4785(2)	26(1)	1
C(40)	2005(3)	3806(2)	4324(2)	28(1)	1
C(41)	2535(3)	4153(2)	3706(2)	29(1)	1
C(42)	3270(2)	6344(2)	3978(2)	23(1)	1
C(43)	3922(2)	5931(2)	4650(2)	24(1)	1
C(44)	4911(3)	6191(2)	4883(2)	31(1)	1
C(45)	5239(3)	6816(2)	4426(2)	42(1)	1
C(46)	4549(3)	7184(2)	3764(2)	36(1)	1
C(47)	1219(2)	8225(2)	1035(2)	21(1)	1
C(48)	704(2)	8676(2)	1552(2)	20(1)	1
C(49)	-302(3)	9342(2)	1365(2)	27(1)	1
C(50)	-710(3)	9705(2)	1860(2)	34(1)	1
C(51)	-117(3)	9386(2)	2555(2)	40(1)	1
C(52)	865(3)	8713(2)	2720(2)	31(1)	1
C(53)	2286(3)	8554(2)	602(2)	26(1)	1
C(54)	2410(3)	9287(2)	456(2)	29(1)	1
C(55)	3423(3)	9484(2)	54(2)	42(1)	1
C(56)	4241(3)	8951(2)	-194(2)	46(1)	1
C(57)	4083(3)	8235(2)	-19(2)	35(1)	1
C(58)	5875(3)	6333(2)	467(2)	35(1)	1
C(59)	6648(3)	5723(2)	1121(2)	41(1)	1
C(62)	4873(3)	7365(2)	1863(2)	28(1)	1
C(63)	6182(3)	7419(2)	1587(2)	39(1)	1
C(60A)	6180(30)	4962(14)	3441(16)	10(3)	0.403(9)
C(61A)	7281(11)	5245(9)	3624(7)	38(3)	0.403(9)
C(60B)	6350(30)	4905(13)	3514(13)	41(6)	0.597(9)
C(61B)	6888(9)	5603(6)	3380(5)	51(2)	0.597(9)

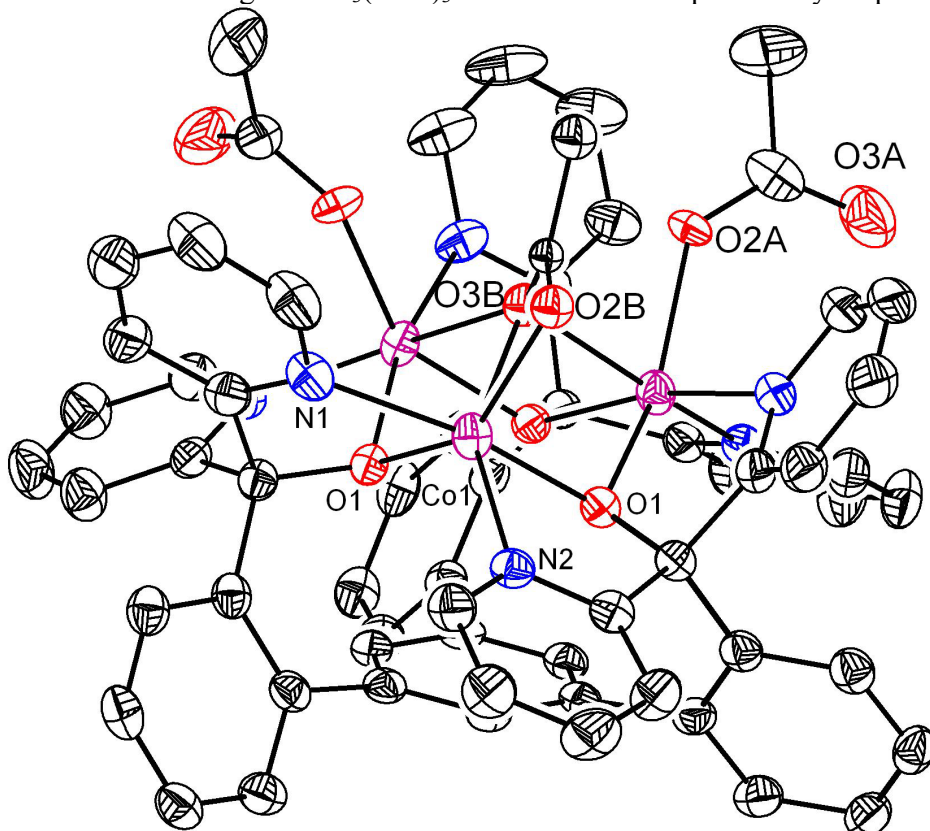
Table S5. Anisotropic displacement parameters ($\text{\AA}^2 \times 10^4$) for LFe₃(OAc)₃. The anisotropic displacement factor exponent takes the form: $-2\pi^2 [h^2 a^{*2} U^{11} + \dots + 2 h k a^{*} b^{*} U^{12}]$.

	U ¹¹	U ²²	U ³³	U ²³	U ¹³	U ¹²
Fe(1)	135(2)	290(3)	248(3)	-135(2)	59(2)	-103(2)
Fe(2)	114(2)	327(3)	242(3)	-146(2)	-10(2)	-9(2)
Fe(3)	126(2)	255(3)	256(3)	-100(2)	2(2)	-53(2)
O(1)	114(9)	280(12)	249(12)	-135(9)	22(8)	-69(8)
O(2)	115(9)	271(11)	203(11)	-108(9)	28(8)	-54(8)
O(3)	126(9)	190(11)	201(11)	-50(9)	5(8)	-49(8)
O(4)	213(11)	474(15)	420(14)	-285(12)	164(10)	-143(10)
O(5)	364(13)	637(18)	682(18)	-373(15)	322(13)	-345(13)
O(8)	224(11)	354(13)	320(13)	-178(11)	52(9)	-114(10)
O(9)	114(9)	437(14)	435(14)	-271(12)	14(9)	-91(9)
O(6A)	200(30)	260(40)	300(40)	-80(30)	-60(30)	-90(30)
O(7A)	570(60)	270(40)	310(40)	20(30)	-60(30)	-140(40)
O(6B)	200(20)	610(50)	310(30)	-250(30)	-27(19)	-40(20)
O(7B)	360(30)	390(30)	420(30)	-50(20)	-70(20)	130(20)

N(1)	115(11)	331(15)	221(14)	-128(12)	31(10)	-90(10)
N(2)	150(11)	301(15)	214(14)	-128(11)	30(10)	-58(10)
N(3)	164(11)	267(14)	208(14)	-107(11)	-83(10)	24(10)
N(4)	184(12)	229(14)	287(15)	-80(12)	-58(11)	-57(11)
N(5)	199(12)	301(15)	308(16)	-148(13)	56(11)	-120(11)
N(6)	214(13)	382(17)	266(15)	-93(13)	55(11)	-159(12)
C(1)	84(12)	294(18)	253(17)	-118(14)	-2(11)	-72(12)
C(2)	65(11)	221(16)	209(16)	-70(13)	24(11)	-79(11)
C(3)	65(12)	282(17)	213(16)	-35(13)	8(11)	-66(11)
C(4)	80(12)	275(17)	190(16)	-72(13)	42(11)	-61(11)
C(5)	78(12)	232(16)	289(18)	-80(14)	24(11)	-36(11)
C(6)	47(11)	265(17)	243(17)	-69(13)	-7(11)	-78(11)
C(7)	156(13)	266(17)	157(15)	-61(13)	-12(11)	-96(12)
C(8)	193(15)	400(20)	243(18)	-91(15)	16(13)	-123(14)
C(9)	282(16)	214(17)	271(18)	-21(14)	-12(13)	-106(13)
C(10)	245(16)	261(18)	293(18)	-64(14)	1(13)	-83(14)
C(11)	170(14)	222(17)	275(18)	-73(14)	-43(12)	-36(12)
C(12)	134(13)	237(16)	193(16)	-72(13)	-22(11)	-62(12)
C(13)	151(13)	216(16)	183(16)	-65(13)	19(11)	-82(12)
C(14)	138(13)	254(17)	296(18)	-78(14)	5(12)	-23(12)
C(15)	236(16)	280(18)	350(20)	-127(15)	136(14)	9(13)
C(16)	300(17)	332(19)	244(18)	-130(15)	64(14)	-61(14)
C(17)	219(15)	314(18)	248(18)	-156(15)	12(13)	-69(13)
C(18)	151(13)	242(17)	288(18)	-79(14)	69(12)	-40(12)
C(19)	117(12)	257(17)	184(16)	-63(13)	33(11)	-46(12)
C(20)	160(14)	286(17)	246(17)	-74(14)	28(12)	-78(12)
C(21)	218(15)	360(20)	258(18)	-84(15)	-51(13)	-88(14)
C(22)	296(17)	380(20)	214(18)	8(15)	33(14)	-103(15)
C(23)	215(15)	294(18)	276(18)	-96(15)	27(13)	-131(13)
C(24)	134(13)	223(16)	223(17)	-90(13)	-6(11)	-21(12)
C(25)	161(13)	203(16)	202(16)	-116(13)	20(11)	-67(11)
C(26)	108(12)	193(16)	234(16)	-93(13)	36(11)	-60(11)
C(27)	156(13)	280(17)	215(17)	-94(14)	22(12)	-71(12)
C(28)	185(14)	380(20)	216(17)	-162(15)	32(12)	-109(13)
C(29)	181(14)	360(20)	208(17)	-97(14)	10(12)	-78(13)
C(30)	181(14)	233(17)	232(17)	-55(14)	40(12)	-50(12)
C(31)	123(13)	242(16)	277(17)	-171(14)	37(12)	-61(12)
C(32)	198(15)	316(18)	268(18)	-121(15)	5(13)	-57(13)
C(33)	166(14)	380(20)	360(20)	-158(16)	61(14)	-21(13)
C(34)	209(15)	380(20)	340(20)	-168(16)	24(14)	52(14)
C(35)	212(15)	390(20)	253(18)	-124(15)	-22(13)	12(14)
C(36)	162(13)	290(17)	206(17)	-135(14)	-22(12)	-44(12)
C(37)	112(13)	239(16)	216(16)	-67(13)	-49(11)	-17(12)
C(38)	138(13)	281(18)	310(18)	-160(15)	14(12)	-14(12)
C(39)	166(14)	290(18)	301(19)	-64(15)	-24(13)	-44(13)
C(40)	249(16)	252(18)	350(20)	-108(15)	-72(14)	-51(13)
C(41)	287(16)	276(19)	302(19)	-144(15)	-95(14)	6(14)
C(42)	157(14)	287(18)	318(19)	-184(15)	25(13)	-74(13)
C(43)	176(14)	200(16)	337(19)	-104(14)	-34(13)	-12(12)
C(44)	285(17)	257(18)	360(20)	-90(16)	-137(15)	-3(14)
C(45)	310(18)	340(20)	590(30)	-84(19)	-219(17)	-119(16)
C(46)	361(19)	228(18)	460(20)	-46(16)	-97(16)	-123(15)
C(47)	167(14)	228(17)	245(17)	-81(13)	-2(12)	-87(12)
C(48)	158(13)	223(16)	253(17)	-74(13)	42(12)	-94(12)

C(49)	244(15)	242(17)	292(19)	-43(14)	9(13)	-75(13)
C(50)	342(18)	218(18)	410(20)	-95(16)	35(16)	-2(14)
C(51)	450(20)	390(20)	420(20)	-261(18)	83(17)	-62(17)
C(52)	270(16)	370(20)	340(20)	-201(16)	-5(14)	-74(15)
C(53)	164(14)	320(19)	276(18)	-38(15)	5(13)	-117(13)
C(54)	233(15)	250(18)	370(20)	-32(15)	24(14)	-126(14)
C(55)	357(19)	310(20)	520(20)	42(18)	-18(17)	-200(17)
C(56)	327(19)	530(30)	490(20)	-20(20)	192(17)	-207(18)
C(57)	243(16)	480(20)	330(20)	-82(17)	126(14)	-174(16)
C(58)	245(16)	490(20)	540(20)	-410(20)	160(16)	-193(16)
C(59)	233(16)	480(20)	610(30)	-310(20)	47(17)	-98(16)
C(62)	153(14)	460(20)	265(18)	-146(16)	22(13)	-77(14)
C(63)	191(16)	580(20)	510(20)	-300(20)	60(15)	-160(16)
C(60A)	200(80)	100(60)	20(60)	0(40)	-40(50)	-100(60)
C(61A)	170(50)	800(110)	240(60)	-260(70)	40(40)	-100(50)
C(60B)	330(80)	640(100)	220(90)	-180(70)	50(70)	-20(60)
C(61B)	390(60)	740(80)	540(60)	-240(50)	50(40)	-350(50)

Figure S12. Structural drawing of $\text{LCo}_3(\text{OAc})_3$ with 50% thermal probability ellipsoids.



Special refinement details for $\text{LCo}_3(\text{OAc})_3$. Crystals were mounted on a glass fiber using Paratone oil then placed on the diffractometer under a nitrogen stream at 100K. The molecule sits around a 3-fold axis. The bound acetate displays two bonding modes, both mono- and bidentate. The populations of both modes were refined to a ratio of 73:27 respectively. The bi-

dentate mode places one oxygen and the methyl group nearly on the 3-fold axis and so can not be present more than 1/3rd of the time. A refined population of 27% suggest a mixture in the crystal with a species where all three acetate ligands are mono-dentate. Refinement of F² against ALL reflections. The weighted R-factor (wR) and goodness of fit (S) are based on F², conventional R-factors (R) are based on F, with F set to zero for negative F². The threshold expression of F² > 2s(F²) is used only for calculating R-factors(gt) etc. and is not relevant to the choice of reflections for refinement. R-factors based on F² are statistically about twice as large as those based on F, and R-factors based on ALL data will be even larger. All esds (except the esd in the dihedral angle between two l.s. planes) are estimated using the full covariance matrix. The cell esds are taken into account individually in the estimation of esds in distances, angles and torsion angles; correlations between esds in cell parameters are only used when they are defined by crystal symmetry. An approximate (isotropic) treatment of cell esds is used for estimating esds involving l.s. planes.

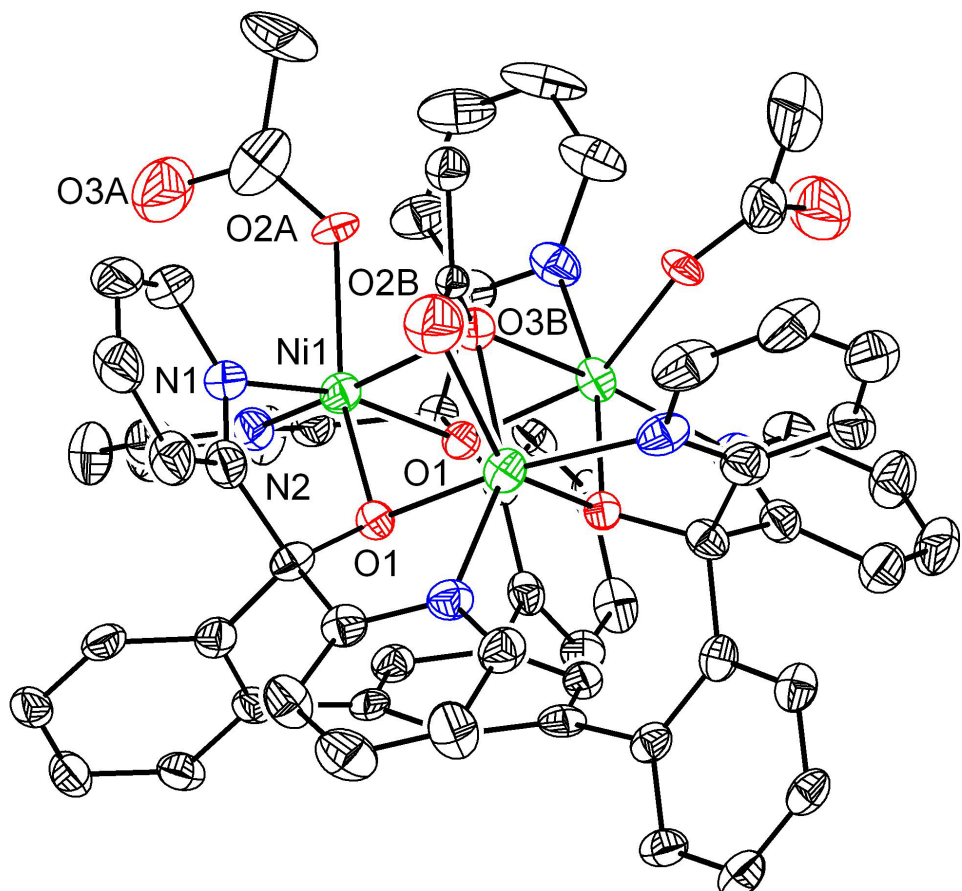
Table S6. Atomic coordinates (x 10⁴) and equivalent isotropic displacement parameters (Å² x 10³) for LCo₃(OAc)₃. U(eq) is defined as the trace of the orthogonalized U^{ij} tensor.

	x	y	z	U _{eq}	Occ
Co(1)	2781(1)	5636(1)	9358(1)	26(1)	1
O(1)	3780(1)	6185(1)	8442(2)	23(1)	1
N(1)	1628(1)	5181(1)	10019(2)	33(1)	1
N(2)	2808(1)	4780(1)	8375(2)	26(1)	1
C(1)	2760(1)	6819(1)	5878(2)	26(1)	1
C(2)	2604(1)	6090(1)	5902(2)	25(1)	1
C(3)	1830(1)	5458(1)	6017(2)	26(1)	1
C(4)	1556(1)	4942(1)	5044(3)	32(1)	1
C(5)	852(1)	4314(1)	5101(3)	33(1)	1
C(6)	417(1)	4204(1)	6173(3)	33(1)	1
C(7)	676(1)	4709(1)	7141(3)	31(1)	1
C(8)	1381(1)	5350(1)	7105(2)	26(1)	1
C(9)	1648(1)	5896(1)	8221(2)	24(1)	1
C(10)	1262(2)	5475(1)	9450(2)	30(1)	1
C(11)	612(1)	5402(2)	9945(3)	37(1)	1
C(12)	342(2)	5025(2)	11066(3)	48(1)	1
C(13)	714(2)	4731(2)	11669(3)	53(1)	1
C(14)	1346(2)	4808(2)	11119(3)	46(1)	1
C(15)	3480(1)	4942(1)	7967(2)	27(1)	1
C(16)	3610(2)	4423(1)	7378(3)	38(1)	1
C(17)	3005(2)	3710(2)	7201(3)	45(1)	1
C(18)	2317(2)	3545(2)	7603(3)	41(1)	1
C(19)	2237(2)	4097(1)	8193(3)	34(1)	1
O(2A)	3058(4)	5351(4)	11064(6)	30(1)	0.727(2)
O(3A)	2407(2)	4109(2)	11217(3)	66(1)	0.727(2)
C(20A)	2883(2)	4730(2)	11604(4)	41(1)	0.727(2)
C(21A)	3207(3)	4751(3)	12899(5)	60(1)	0.727(2)
O(2B)	2357(13)	6902(16)	11200(20)	62(8)	0.273(2)
O(3B)	3221(4)	6685(6)	10502(3)	5(1)	0.273(2)
C(20B)	2860(4)	6733(4)	11391(7)	18(2)	0.273(2)
C(21B)	2981(5)	6542(6)	12685(8)	30(2)	0.273(2)

Table S7. Anisotropic displacement parameters ($\text{\AA}^2 \times 10^4$) for $\text{LCo}_3(\text{OAc})_3$. The anisotropic displacement factor exponent takes the form: $-2\pi^2 [h^2 a^{*2} U^{11} + \dots + 2 h k a^{*} b^{*} U^{12}]$

	U^{11}	U^{22}	U^{33}	U^{23}	U^{13}	U^{12}
Co(1)	246(2)	219(2)	329(2)	26(2)	-8(2)	121(2)
O(1)	247(8)	212(8)	248(9)	0(7)	-18(7)	119(7)
N(1)	300(11)	291(11)	301(12)	64(9)	-17(10)	84(9)
N(2)	286(10)	248(10)	230(11)	4(8)	4(8)	114(8)
C(1)	274(12)	333(13)	187(12)	-7(10)	-1(9)	162(10)
C(2)	273(12)	289(12)	154(11)	26(9)	9(9)	123(10)
C(3)	281(12)	282(12)	238(13)	-2(10)	-44(9)	154(10)
C(4)	378(14)	345(14)	269(14)	-25(11)	-37(11)	199(12)
C(5)	355(14)	296(13)	343(15)	-57(11)	-92(11)	162(11)
C(6)	288(13)	252(12)	449(16)	-15(11)	-103(12)	131(11)
C(7)	288(13)	315(13)	345(14)	47(11)	5(11)	163(11)
C(8)	260(12)	275(12)	286(13)	35(10)	-17(10)	155(10)
C(9)	241(12)	258(11)	247(13)	21(9)	13(9)	132(10)
C(10)	281(13)	271(12)	277(14)	7(11)	13(10)	85(11)
C(11)	294(13)	397(15)	336(16)	-2(12)	48(11)	109(11)
C(12)	288(14)	572(19)	383(17)	39(15)	65(13)	71(14)
C(13)	337(15)	600(20)	317(16)	175(15)	22(13)	-27(14)
C(14)	370(16)	430(16)	377(17)	135(13)	-56(13)	57(13)
C(15)	309(13)	244(11)	255(13)	25(10)	-11(10)	141(10)
C(16)	344(14)	272(13)	465(18)	-30(12)	61(12)	122(11)
C(17)	523(18)	297(14)	530(19)	-105(13)	42(15)	198(14)
C(18)	381(15)	249(13)	503(19)	-59(12)	5(13)	79(12)
C(19)	311(13)	281(13)	353(15)	-6(11)	6(11)	99(11)
O(2A)	330(20)	308(18)	219(18)	94(15)	-19(13)	133(16)
O(3A)	1020(30)	344(17)	510(20)	45(14)	30(19)	272(18)
C(20A)	510(20)	490(20)	350(20)	111(19)	111(18)	350(20)
C(21A)	650(30)	830(40)	580(30)	10(30)	-220(30)	560(30)

Figure S13. Structural drawing of $\text{LNi}_3(\text{OAc})_3$ with 50% thermal probability ellipsoids.



Special refinement details for $\text{LNi}_3(\text{OAc})_3$. Crystals were mounted on a glass fiber using Paratone oil then placed on the diffractometer under a nitrogen stream at 100K. The molecule sits around a 3-fold axis. The bound acetate displays two bonding modes, both mono- and bi-dentate. The populations of both modes were refined to a ratio of 74:26 respectively. The bi-dentate mode places one oxygen and the methyl group nearly on the 3-fold axis and so can not be present more than 1/3rd of the time. A refined population of 26% suggest a mixture in the crystal with a species where all three acetate ligands are mono-dentate. Refinement of F^2 against ALL reflections. The weighted R-factor (wR) and goodness of fit (S) are based on F^2 , conventional R-factors (R) are based on F , with F set to zero for negative F^2 . The threshold expression of $F^2 > 2s(F^2)$ is used only for calculating R-factors(gt) etc. and is not relevant to the choice of reflections for refinement. R-factors based on F^2 are statistically about twice as large as those based on F , and R-factors based on ALL data will be even larger. All esds (except the esd in the dihedral angle between two l.s. planes) are estimated using the full covariance matrix. The cell esds are taken into account individually in the estimation of esds in distances, angles and torsion angles; correlations between esds in cell parameters are only used when they are defined by crystal symmetry. An approximate (isotropic) treatment of cell esds is used for estimating esds involving l.s. planes.

Table S8. Atomic coordinates ($\times 10^4$) and equivalent isotropic displacement parameters ($\text{\AA}^2 \times 10^3$) for $\text{LNi}_3(\text{OAc})_3$. U(eq) is defined as the trace of the orthogonalized U^{ij} tensor.

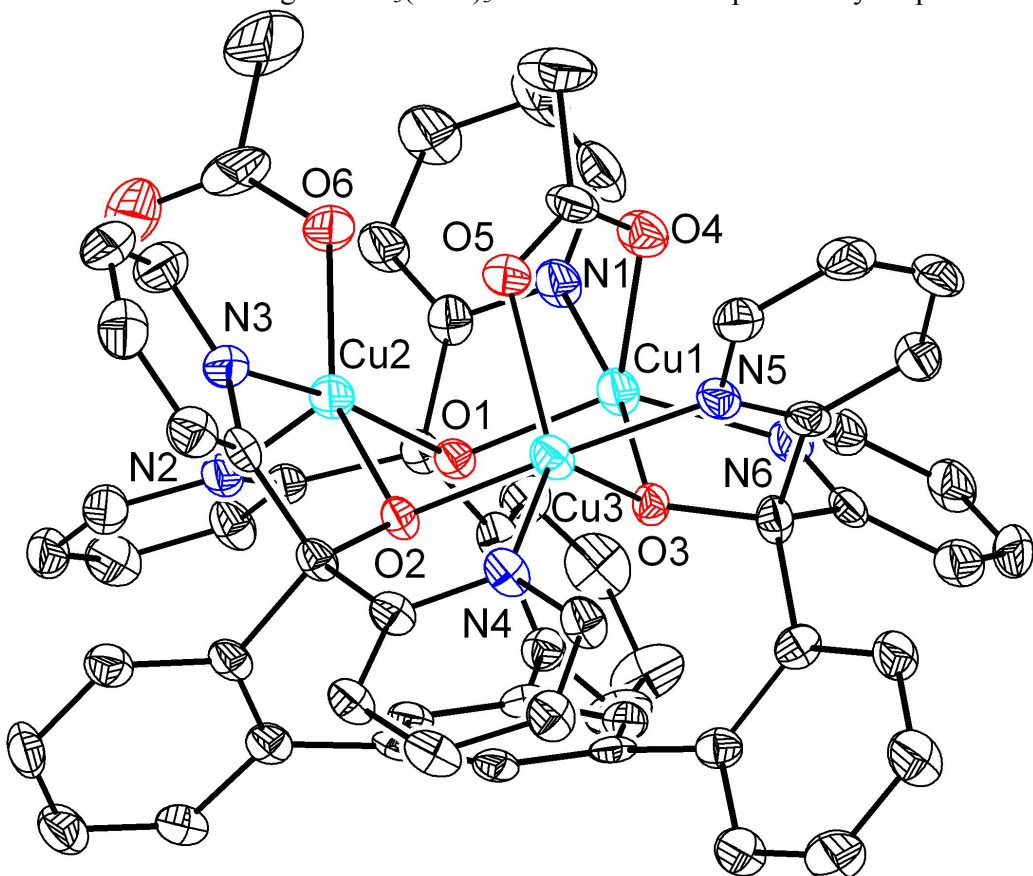
	x	y	z	U _{eq}	Occ
Ni(1)	7212(1)	4357(1)	643(1)	27(1)	1
O(1)	6222(1)	3797(1)	1598(2)	22(1)	1
N(1)	8318(2)	4786(2)	-42(3)	33(1)	1
N(2)	7215(1)	5198(1)	1645(2)	29(1)	1
C(1)	7243(2)	3184(2)	4128(2)	26(1)	1
C(2)	7403(2)	3913(2)	4115(3)	25(1)	1
C(3)	8184(2)	4557(2)	3974(3)	25(1)	1
C(4)	8466(2)	5074(2)	4933(3)	31(1)	1
C(5)	9175(2)	5703(2)	4860(3)	34(1)	1
C(6)	9611(2)	5818(2)	3780(3)	30(1)	1
C(7)	9331(2)	5300(2)	2833(3)	29(1)	1
C(8)	8620(2)	4660(2)	2877(3)	26(1)	1
C(9)	8331(2)	4106(2)	1774(3)	26(1)	1
C(10)	8709(2)	4524(2)	551(3)	34(1)	1
C(11)	9383(2)	4628(2)	50(3)	40(1)	1
C(12)	9643(2)	5000(2)	-1072(3)	53(1)	1
C(13)	9245(2)	5272(2)	-1688(3)	57(1)	1
C(14)	8592(2)	5169(2)	-1163(3)	50(1)	1
C(15)	6526(2)	5048(2)	2024(3)	29(1)	1
C(16)	6405(2)	5586(2)	2571(3)	38(1)	1
C(17)	7028(2)	6295(2)	2764(4)	48(1)	1
C(18)	7726(2)	6454(2)	2396(3)	42(1)	1
C(19)	7790(2)	5875(2)	1824(3)	34(1)	1
O(2A)	6859(3)	4648(3)	-966(4)	27(1)	0.741(2)
O(3A)	7563(2)	5889(2)	-1154(4)	72(1)	0.741(2)
C(20A)	7072(3)	5260(3)	-1553(6)	53(2)	0.741(2)
C(21A)	6790(3)	5265(3)	-2908(5)	65(2)	0.741(2)
O(2B)	7666(10)	3181(10)	-1321(15)	54(6)	0.259(2)
O(3B)	6790(6)	3330(10)	-520(4)	2(2)	0.259(2)
C(20B)	7163(6)	3318(6)	-1391(10)	17(2)	0.259(2)
C(21B)	7019(6)	3471(8)	-2598(10)	30(3)	0.259(2)

Table S9. Anisotropic displacement parameters ($\text{\AA}^2 \times 10^4$) for $\text{LNi}_3(\text{OAc})_3$. The anisotropic displacement factor exponent takes the form: $-2\pi^2 [h^2 a^*{}^2 U^{11} + \dots + 2 h k a^* b^* U^{12}]$

	U ¹¹	U ²²	U ³³	U ²³	U ¹³	U ¹²
Ni(1)	281(2)	244(2)	292(2)	26(2)	-19(2)	134(2)
O(1)	229(12)	213(12)	230(13)	7(10)	7(10)	116(10)
N(1)	367(17)	293(16)	260(16)	27(13)	-46(14)	103(14)
N(2)	299(15)	263(15)	269(16)	-25(12)	-9(13)	109(13)
C(1)	275(18)	344(18)	201(17)	-8(14)	-13(13)	186(16)
C(2)	322(18)	256(17)	122(15)	28(13)	21(13)	106(15)
C(3)	287(18)	244(17)	255(18)	-4(14)	-64(14)	157(14)
C(4)	380(20)	333(19)	232(18)	-38(15)	-64(15)	198(17)
C(5)	322(19)	275(18)	400(20)	-49(16)	-132(16)	135(16)
C(6)	300(18)	257(18)	350(20)	-9(16)	-115(16)	150(16)

C(7)	282(19)	317(19)	281(18)	117(15)	3(15)	150(16)
C(8)	258(18)	252(17)	315(19)	42(15)	-19(15)	153(15)
C(9)	316(19)	274(17)	221(18)	42(13)	50(14)	173(15)
C(10)	310(20)	298(19)	330(20)	-48(16)	-2(15)	88(17)
C(11)	280(19)	430(20)	370(20)	-29(18)	79(17)	89(17)
C(12)	270(20)	660(30)	380(20)	-10(20)	68(18)	20(20)
C(13)	340(20)	750(30)	240(20)	180(20)	31(17)	-10(20)
C(14)	510(30)	430(20)	310(20)	104(18)	-24(19)	70(20)
C(15)	331(19)	273(18)	271(19)	12(14)	-21(15)	162(16)
C(16)	330(20)	266(19)	490(20)	-3(17)	106(18)	111(17)
C(17)	600(30)	310(20)	540(30)	-103(18)	40(20)	240(20)
C(18)	360(20)	290(20)	590(30)	-38(18)	60(18)	134(17)
C(19)	292(19)	330(20)	320(20)	4(16)	-9(16)	92(16)
O(2A)	350(20)	310(20)	190(20)	100(20)	18(18)	192(19)
O(3A)	1060(40)	420(20)	580(30)	-10(20)	20(20)	280(20)
C(20A)	560(40)	500(40)	690(40)	190(30)	270(30)	380(30)
C(21A)	770(40)	820(40)	640(40)	-190(30)	-460(30)	610(40)

Figure S14. Structural drawing of $\text{LCu}_3(\text{OAc})_3$ with 50% thermal probability ellipsoids.



Special refinement details for $\text{LCu}_3(\text{OAc})_3$. Crystals were mounted on a glass fiber using Paratone oil then placed on the diffractometer under a nitrogen stream at 100K. Presumably the solvent region of the crystal contains an acetate which would balance the charge on the Cu complex. Approximately 32% of the unit cell volume contains potential solvent. Electron

density in this space is poorly defined suggesting disorder and a suitable solvent model was not obtained. SQUEEZE⁴ was employed to produce a bulk solvent correction which accounted for 964 electrons which is a good fit to two chloroform and one acetate per unit cell. Refinement of F^2 against ALL reflections. The weighted R-factor (wR) and goodness of fit (S) are based on F^2 , conventional R-factors (R) are based on F, with F set to zero for negative F^2 . The threshold expression of $F^2 > 2\sigma(F^2)$ is used only for calculating R-factors(gt) etc. and is not relevant to the choice of reflections for refinement. R-factors based on F^2 are statistically about twice as large as those based on F, and R-factors based on ALL data will be even larger. All esds (except the esd in the dihedral angle between two l.s. planes) are estimated using the full covariance matrix. The cell esds are taken into account individually in the estimation of esds in distances, angles and torsion angles; correlations between esds in cell parameters are only used when they are defined by crystal symmetry. An approximate (isotropic) treatment of cell esds is used for estimating esds involving l.s. planes.

Table S10. Atomic coordinates (x 10⁴) and equivalent isotropic displacement parameters (Å² × 10³) for LCu₃(OAc)₃. U(eq) is defined as the trace of the orthogonalized U^{ij} tensor.

	x	y	z	U _{eq}
Cu(1)	3111(1)	5800(1)	1289(1)	25(1)
Cu(2)	4625(1)	6570(1)	1052(1)	25(1)
Cu(3)	3921(1)	6865(1)	1838(1)	24(1)
O(1)	3605(1)	6386(1)	929(1)	20(1)
O(2)	4266(1)	7299(1)	1384(1)	21(1)
O(3)	2984(1)	6595(1)	1615(1)	21(1)
O(4)	3704(2)	5209(1)	1675(1)	29(1)
O(5)	4571(2)	5997(1)	1797(1)	30(1)
O(6)	4951(2)	5606(1)	982(1)	33(1)
O(7)	5721(2)	5748(2)	515(1)	52(1)
N(1)	3335(2)	5069(2)	905(1)	28(1)
N(2)	4520(2)	6828(2)	457(1)	26(1)
N(3)	5554(2)	6946(2)	1262(1)	27(1)
N(4)	4143(2)	7822(2)	2038(1)	24(1)
N(5)	3480(2)	6394(2)	2285(1)	24(1)
N(6)	2095(2)	5631(2)	1445(1)	24(1)
C(1)	2196(2)	7444(2)	1158(1)	22(1)
C(2)	2514(2)	7367(2)	816(1)	20(1)
C(3)	3097(2)	7763(2)	734(1)	21(1)
C(4)	3399(2)	8207(2)	997(1)	21(1)
C(5)	3079(2)	8283(2)	1342(1)	21(1)
C(6)	2480(2)	7883(2)	1428(1)	20(1)
C(7)	2263(2)	6801(2)	567(1)	23(1)
C(8)	1556(2)	6801(2)	464(1)	39(1)
C(9)	1242(3)	6292(3)	239(1)	45(1)
C(10)	1666(3)	5768(3)	118(1)	41(1)
C(11)	2367(2)	5735(2)	222(1)	31(1)
C(12)	2682(2)	6243(2)	451(1)	23(1)
C(13)	4093(2)	8538(2)	916(1)	22(1)
C(14)	4142(2)	8998(2)	613(1)	27(1)
C(15)	4762(2)	9328(2)	514(1)	33(1)
C(16)	5367(2)	9199(2)	712(1)	33(1)

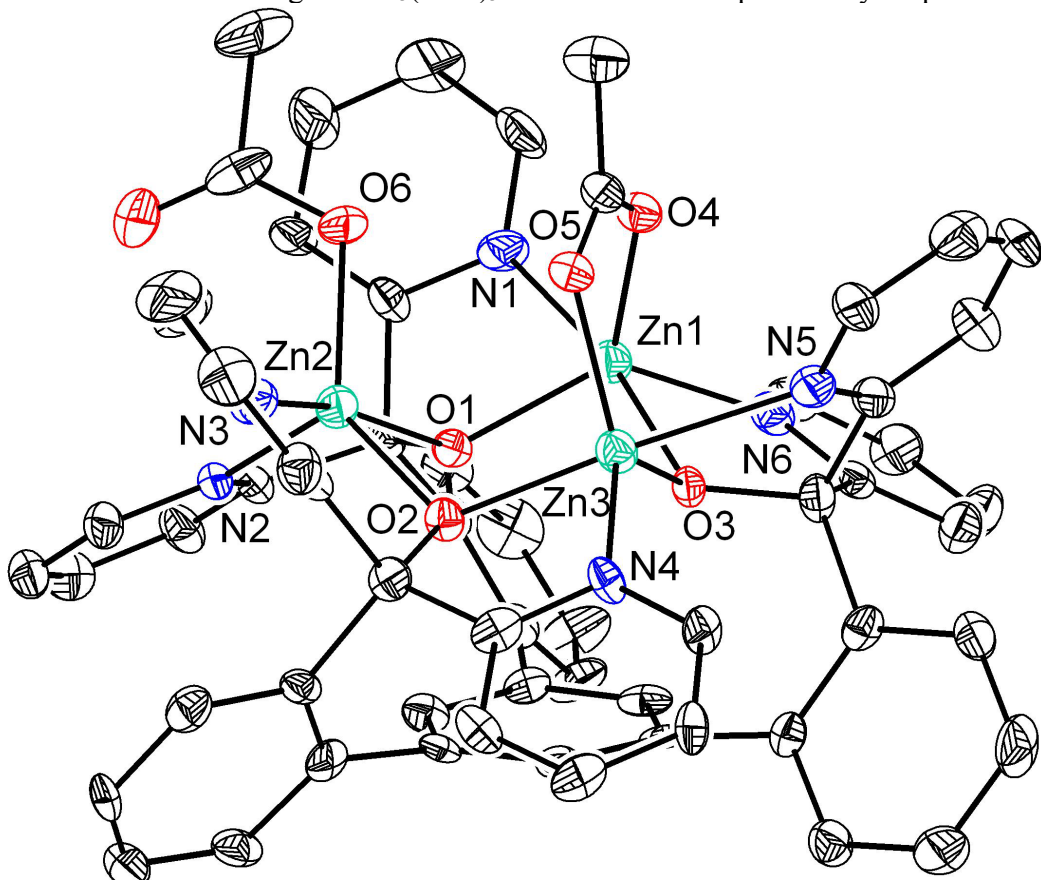
C(17)	5350(2)	8735(2)	1011(1)	27(1)
C(18)	4717(2)	8390(2)	1113(1)	23(1)
C(19)	2219(2)	7868(2)	1815(1)	23(1)
C(20)	2021(2)	8504(2)	1979(1)	31(1)
C(21)	1791(2)	8531(2)	2338(1)	41(1)
C(22)	1726(3)	7921(2)	2544(1)	40(1)
C(23)	1918(2)	7291(2)	2387(1)	32(1)
C(24)	2173(2)	7244(2)	2025(1)	23(1)
C(25)	3466(2)	6138(2)	567(1)	22(1)
C(26)	4744(2)	7857(2)	1446(1)	21(1)
C(27)	2463(2)	6510(2)	1888(1)	24(1)
C(28)	3598(2)	5343(2)	586(1)	25(1)
C(29)	3898(2)	4926(2)	314(1)	37(1)
C(30)	3919(3)	4213(2)	368(1)	50(2)
C(31)	3650(3)	3930(2)	694(1)	53(2)
C(32)	3377(2)	4369(2)	958(1)	42(1)
C(33)	3956(2)	6525(2)	301(1)	23(1)
C(34)	3813(2)	6588(2)	-72(1)	28(1)
C(35)	4249(3)	6985(2)	-290(1)	36(1)
C(36)	4829(2)	7309(2)	-127(1)	36(1)
C(37)	4949(2)	7213(2)	244(1)	30(1)
C(38)	5477(2)	7529(2)	1473(1)	23(1)
C(39)	6035(2)	7788(2)	1680(1)	31(1)
C(40)	6686(2)	7455(3)	1674(1)	36(1)
C(41)	6748(2)	6859(3)	1456(1)	41(1)
C(42)	6171(3)	6619(2)	1253(1)	40(1)
C(43)	4523(2)	8220(2)	1807(1)	23(1)
C(44)	4662(2)	8908(2)	1891(1)	26(1)
C(45)	4362(2)	9200(2)	2205(1)	28(1)
C(46)	3941(2)	8801(2)	2427(1)	28(1)
C(47)	3859(2)	8106(2)	2339(1)	28(1)
C(48)	2824(2)	6152(2)	2224(1)	22(1)
C(49)	2515(2)	5653(2)	2451(1)	30(1)
C(50)	2884(3)	5420(2)	2755(1)	38(1)
C(51)	3548(3)	5691(2)	2820(1)	36(1)
C(52)	3834(2)	6168(2)	2581(1)	28(1)
C(53)	1873(2)	6052(2)	1724(1)	22(1)
C(54)	1173(2)	6079(2)	1830(1)	30(1)
C(55)	681(2)	5670(2)	1644(1)	34(1)
C(56)	907(2)	5252(2)	1348(1)	33(1)
C(57)	1611(2)	5245(2)	1264(1)	29(1)
C(58)	4303(3)	5370(2)	1774(1)	33(1)
C(59)	4803(2)	4790(2)	1879(1)	57(2)
C(60)	5411(3)	5393(3)	743(2)	44(1)
C(61)	5557(3)	4634(3)	773(2)	103(3)

Table S11. Anisotropic displacement parameters ($\text{\AA}^2 \times 10^4$) for $\text{LCu}_3(\text{OAc})_3$. The anisotropic displacement factor exponent takes the form: $-2\pi^2 [h^2 a^{*2} U^{11} + \dots + 2 h k a^{*} b^{*} U^{12}]$.

	U^{11}	U^{22}	U^{33}	U^{23}	U^{13}	U^{12}
Cu(1)	320(3)	188(3)	248(3)	-42(3)	73(3)	-39(3)
Cu(2)	287(3)	185(3)	276(3)	-36(2)	42(3)	-7(3)
Cu(3)	316(3)	195(3)	220(3)	0(2)	21(3)	-25(3)
O(1)	270(18)	157(17)	180(16)	-21(12)	35(13)	-2(13)
O(2)	252(17)	186(17)	183(16)	18(12)	30(13)	-34(14)
O(3)	230(17)	181(16)	211(15)	-24(13)	63(13)	-21(14)
O(4)	300(20)	227(19)	358(19)	14(14)	-38(16)	-37(16)
O(5)	330(20)	199(18)	376(18)	20(14)	60(16)	33(15)
O(6)	370(20)	190(18)	430(20)	-76(15)	95(16)	18(15)
O(7)	540(30)	600(30)	430(20)	-17(19)	201(19)	90(20)
N(1)	370(30)	180(20)	280(20)	-51(17)	66(19)	-44(18)
N(2)	340(20)	160(20)	280(20)	-19(17)	109(19)	-6(19)
N(3)	260(20)	220(20)	340(20)	7(18)	34(18)	18(18)
N(4)	350(20)	210(20)	160(20)	-26(16)	-3(17)	-53(18)
N(5)	330(20)	200(20)	190(20)	17(16)	52(18)	33(19)
N(6)	300(20)	190(20)	250(20)	-10(17)	25(18)	-21(18)
C(1)	200(30)	180(30)	280(30)	10(20)	-40(20)	0(20)
C(2)	220(30)	170(30)	220(30)	-39(19)	-50(20)	60(20)
C(3)	310(30)	130(20)	180(20)	18(19)	20(20)	60(20)
C(4)	270(30)	130(20)	230(20)	87(19)	-10(20)	40(20)
C(5)	280(30)	110(20)	250(20)	-22(19)	0(20)	30(20)
C(6)	250(30)	140(20)	220(30)	-6(19)	-10(20)	100(20)
C(7)	210(30)	240(30)	240(20)	0(20)	-20(20)	0(20)
C(8)	430(30)	330(30)	400(30)	-110(20)	-50(30)	140(30)
C(9)	360(30)	460(40)	520(30)	-230(30)	-160(30)	70(30)
C(10)	530(40)	390(30)	310(30)	-130(20)	-120(30)	-120(30)
C(11)	380(30)	300(30)	270(30)	-60(20)	60(20)	20(30)
C(12)	300(30)	220(30)	170(20)	-60(20)	20(20)	-70(20)
C(13)	310(30)	160(20)	200(20)	-47(19)	10(20)	0(20)
C(14)	350(30)	210(30)	250(30)	10(20)	-30(20)	40(20)
C(15)	450(30)	290(30)	260(30)	70(20)	40(20)	0(30)
C(16)	350(30)	320(30)	330(30)	70(20)	120(20)	-80(30)
C(17)	330(30)	220(30)	260(30)	0(20)	10(20)	20(20)
C(18)	360(30)	130(20)	190(20)	-32(19)	60(20)	-10(20)
C(19)	240(30)	200(30)	250(30)	-20(20)	-30(20)	10(20)
C(20)	450(30)	260(30)	210(30)	-20(20)	60(20)	30(20)
C(21)	560(40)	260(30)	410(30)	-120(20)	110(30)	70(30)
C(22)	650(40)	310(30)	230(30)	-30(20)	160(30)	20(30)
C(23)	440(30)	260(30)	270(30)	10(20)	140(20)	20(20)
C(24)	270(30)	240(30)	190(20)	-70(20)	10(20)	20(20)
C(25)	320(30)	150(20)	190(20)	-60(20)	80(20)	-30(20)
C(26)	280(30)	140(20)	200(20)	-24(19)	10(20)	-50(20)
C(27)	250(30)	220(30)	240(30)	-20(20)	60(20)	-60(20)
C(28)	290(30)	230(30)	240(30)	-60(20)	20(20)	-60(20)
C(29)	570(40)	180(30)	350(30)	-40(20)	180(30)	0(30)
C(30)	840(40)	220(30)	440(30)	-130(20)	240(30)	0(30)
C(31)	940(50)	130(30)	510(30)	-60(30)	350(30)	-50(30)
C(32)	650(40)	230(30)	390(30)	0(20)	200(30)	-120(30)

C(33)	290(30)	140(20)	260(30)	-50(20)	80(20)	0(20)
C(34)	400(30)	200(30)	230(30)	-30(20)	40(20)	-80(20)
C(35)	520(40)	290(30)	250(30)	-20(20)	50(30)	30(30)
C(36)	390(30)	250(30)	420(30)	0(20)	190(30)	0(20)
C(37)	310(30)	240(30)	350(30)	-50(20)	80(20)	-30(20)
C(38)	260(30)	200(30)	230(30)	60(20)	30(20)	-50(20)
C(39)	370(30)	310(30)	250(30)	0(20)	0(20)	0(30)
C(40)	310(30)	480(40)	290(30)	50(20)	-30(20)	-40(30)
C(41)	260(30)	400(30)	580(30)	50(30)	30(30)	90(30)
C(42)	320(30)	320(30)	570(30)	-30(30)	60(30)	30(30)
C(43)	300(30)	210(30)	170(20)	0(20)	-20(20)	-10(20)
C(44)	350(30)	200(30)	230(30)	20(20)	0(20)	-40(20)
C(45)	430(30)	210(30)	210(30)	-10(20)	-80(20)	-20(20)
C(46)	350(30)	300(30)	190(20)	-20(20)	10(20)	-10(20)
C(47)	370(30)	230(30)	230(20)	-40(20)	30(20)	-70(20)
C(48)	330(30)	160(30)	180(20)	-10(20)	50(20)	70(20)
C(49)	320(30)	280(30)	290(30)	30(20)	30(20)	-10(20)
C(50)	540(40)	280(30)	330(30)	150(20)	140(30)	120(30)
C(51)	390(30)	400(30)	280(30)	100(20)	-30(20)	160(30)
C(52)	320(30)	290(30)	240(30)	10(20)	10(20)	70(20)
C(53)	290(30)	140(20)	230(30)	39(19)	50(20)	-30(20)
C(54)	370(30)	210(30)	320(30)	-40(20)	40(20)	-10(20)
C(55)	250(30)	290(30)	490(30)	20(20)	100(20)	-70(20)
C(56)	380(30)	210(30)	400(30)	-40(20)	50(20)	-100(20)
C(57)	340(30)	190(30)	330(30)	-30(20)	50(20)	-40(20)
C(58)	470(40)	180(30)	330(30)	60(20)	80(30)	80(30)
C(59)	450(40)	240(30)	1030(50)	50(30)	-210(30)	30(30)
C(60)	440(40)	260(30)	600(40)	-250(30)	10(30)	100(30)
C(61)	1010(60)	350(40)	1740(70)	-210(40)	640(50)	180(40)

Figure S15. Structural drawing of $\text{LZn}_3(\text{OAc})_3$ with 50% thermal probability ellipsoids.



Special refinement details for $\text{LZn}_3(\text{OAc})_3$. Crystals were mounted in a loop using oil then placed on the diffractometer under a nitrogen stream at 100K. Presumably the solvent region of the crystal contains an acetate which would balance the charge on the Zn complex. Approximately 31% of the unit cell volume contains potential solvent. Electron density in this space is poorly defined suggesting disorder and a suitable solvent model was not obtained. SQUEEZE⁴ was employed to produce a bulk solvent correction which accounted for 1066 electrons which is a good fit to two chloroform and one acetate per unit cell. Refinement of F^2 against ALL reflections. The weighted R-factor (wR) and goodness of fit (S) are based on F^2 , conventional R-factors (R) are based on F, with F set to zero for negative F^2 . The threshold expression of $F^2 > 2\sigma(F^2)$ is used only for calculating R-factors(gt) etc. and is not relevant to the choice of reflections for refinement. R-factors based on F^2 are statistically about twice as large as those based on F, and R-factors based on ALL data will be even larger. All esds (except the esd in the dihedral angle between two l.s. planes) are estimated using the full covariance matrix. The cell esds are taken into account individually in the estimation of esds in distances, angles and torsion angles; correlations between esds in cell parameters are only used when they are defined by crystal symmetry. An approximate (isotropic) treatment of cell esds is used for estimating esds involving l.s. planes.

Table S12. Atomic coordinates ($\times 10^4$) and equivalent isotropic displacement parameters ($\text{\AA}^2 \times 10^3$) for LZn₃(OAc)₃. U(eq) is defined as the trace of the orthogonalized U^{ij} tensor.

	x	y	z	U _{eq}
Zn(1)	3194(1)	5747(1)	1307(1)	22(1)
Zn(2)	4668(1)	6594(1)	999(1)	22(1)
Zn(3)	3957(1)	6853(1)	1845(1)	22(1)
O(1)	3596(2)	6343(2)	915(1)	18(1)
O(2)	4338(2)	7297(2)	1370(1)	19(1)
O(3)	3044(2)	6602(2)	1660(1)	18(1)
O(4)	3802(2)	5196(2)	1658(1)	24(1)
O(5)	4586(2)	6002(2)	1865(1)	25(1)
O(6)	4991(2)	5607(2)	1064(1)	28(1)
O(7)	5696(2)	5706(2)	569(1)	45(1)
N(1)	3387(2)	4969(2)	854(1)	27(1)
N(2)	4520(2)	6808(2)	445(1)	21(1)
N(3)	5652(2)	7076(2)	1202(1)	28(1)
N(4)	4181(2)	7848(2)	2038(1)	20(1)
N(5)	3457(2)	6394(2)	2357(1)	25(1)
N(6)	2147(2)	5653(2)	1444(1)	23(1)
C(1)	2209(3)	7412(2)	1160(2)	21(2)
C(2)	2523(3)	7338(3)	816(2)	19(1)
C(3)	3090(3)	7740(2)	724(2)	22(2)
C(4)	3390(3)	8190(2)	989(2)	21(1)
C(5)	3085(3)	8264(2)	1339(2)	21(1)
C(6)	2484(3)	7863(2)	1431(2)	21(2)
C(7)	2262(3)	6754(3)	569(2)	23(1)
C(8)	1548(3)	6740(3)	467(2)	36(2)
C(9)	1246(3)	6227(3)	241(2)	38(2)
C(10)	1670(3)	5702(3)	119(2)	38(2)
C(11)	2382(3)	5674(3)	207(1)	28(2)
C(12)	2690(3)	6193(3)	441(2)	23(2)
C(13)	4072(3)	8545(2)	899(2)	21(1)
C(14)	4085(3)	9000(2)	588(2)	26(2)
C(15)	4697(3)	9348(3)	478(2)	29(2)
C(16)	5295(3)	9256(3)	675(2)	29(2)
C(17)	5309(3)	8804(2)	973(2)	25(1)
C(18)	4708(3)	8432(2)	1094(1)	19(1)
C(19)	2227(3)	7869(3)	1821(2)	19(1)
C(20)	2014(3)	8518(3)	1973(2)	27(2)
C(21)	1772(3)	8576(3)	2321(2)	34(2)
C(22)	1734(3)	7972(3)	2542(2)	38(2)
C(23)	1954(3)	7319(3)	2396(2)	30(2)
C(24)	2203(3)	7258(3)	2046(2)	21(2)
C(25)	3484(3)	6107(3)	554(2)	19(1)
C(26)	4764(3)	7890(3)	1428(2)	22(2)
C(27)	2502(3)	6518(3)	1914(2)	23(2)
C(28)	3644(3)	5288(3)	546(2)	23(2)
C(29)	3972(3)	4935(3)	267(2)	33(2)
C(30)	4029(4)	4219(3)	294(2)	53(2)
C(31)	3762(4)	3870(3)	603(2)	65(3)
C(32)	3458(3)	4259(3)	878(2)	44(2)

C(33)	3952(3)	6514(2)	290(2)	19(1)
C(34)	3807(3)	6606(2)	-73(2)	26(2)
C(35)	4234(3)	7025(3)	-280(2)	32(2)
C(36)	4816(3)	7338(3)	-120(2)	33(2)
C(37)	4946(3)	7213(3)	242(2)	25(2)
C(38)	5526(3)	7615(3)	1450(2)	24(2)
C(39)	6053(3)	7860(3)	1688(2)	28(2)
C(40)	6709(3)	7563(3)	1677(2)	37(2)
C(41)	6823(3)	7017(3)	1425(2)	46(2)
C(42)	6289(3)	6790(3)	1189(2)	44(2)
C(43)	4540(3)	8248(3)	1805(2)	22(1)
C(44)	4663(3)	8960(2)	1881(2)	24(1)
C(45)	4387(3)	9253(3)	2196(2)	28(2)
C(46)	3991(3)	8837(3)	2419(2)	25(2)
C(47)	3905(3)	8144(3)	2333(1)	22(1)
C(48)	2815(3)	6138(3)	2258(2)	25(2)
C(49)	2480(3)	5590(3)	2452(2)	32(2)
C(50)	2809(4)	5327(3)	2760(2)	41(2)
C(51)	3454(3)	5612(3)	2866(2)	37(2)
C(52)	3764(3)	6130(3)	2655(2)	30(2)
C(53)	1916(3)	6069(3)	1724(2)	20(1)
C(54)	1224(3)	6097(3)	1822(2)	28(2)
C(55)	752(3)	5712(3)	1622(2)	34(2)
C(56)	960(3)	5302(3)	1326(2)	32(2)
C(57)	1674(3)	5278(2)	1246(2)	28(2)
C(58)	4369(3)	5377(3)	1810(2)	26(2)
C(59)	4826(3)	4784(2)	1939(2)	37(2)
C(60)	5426(4)	5373(3)	817(2)	39(2)
C(61)	5586(4)	4581(3)	862(2)	86(3)

Table S13. Anisotropic displacement parameters ($\text{\AA}^2 \times 10^4$) for $\text{LZn}_3(\text{OAc})_3$. The anisotropic displacement factor exponent takes the form: $-2\pi^2 [h^2 a^{*2} U^{11} + \dots + 2 h k a^{*} b^{*} U^{12}]$.

	U ¹¹	U ²²	U ³³	U ²³	U ¹³	U ¹²
Zn(1)	250(4)	185(3)	210(4)	-11(3)	32(4)	-18(3)
Zn(2)	245(4)	197(3)	226(4)	-22(3)	26(4)	-7(3)
Zn(3)	249(4)	203(3)	212(4)	-4(3)	14(4)	-22(3)
O(1)	220(20)	164(19)	140(20)	-15(16)	-7(19)	6(16)
O(2)	200(20)	180(19)	190(30)	-23(17)	7(19)	-46(17)
O(3)	200(20)	178(19)	160(20)	-1(17)	46(19)	-23(18)
O(4)	290(30)	180(20)	250(30)	12(17)	20(20)	13(19)
O(5)	290(20)	180(20)	290(30)	30(18)	40(20)	10(19)
O(6)	320(30)	160(20)	360(30)	-20(18)	60(20)	43(18)
O(7)	510(30)	480(30)	350(30)	20(20)	200(30)	120(20)
N(1)	350(30)	160(30)	300(40)	-60(20)	10(30)	20(20)
N(2)	260(30)	170(20)	200(30)	30(20)	80(20)	30(20)
N(3)	210(30)	250(30)	380(40)	0(20)	20(30)	0(20)
N(4)	260(30)	210(30)	130(30)	20(20)	0(20)	-70(20)
N(5)	300(30)	200(30)	240(30)	-20(20)	30(30)	20(20)
N(6)	280(30)	180(30)	240(30)	10(20)	10(30)	-40(20)
C(1)	140(30)	130(30)	350(40)	-10(30)	-120(30)	10(30)

C(2)	180(40)	180(30)	210(40)	-40(30)	-60(30)	30(30)
C(3)	270(40)	180(30)	200(40)	0(30)	-40(30)	0(30)
C(4)	240(40)	120(30)	280(40)	90(30)	30(30)	30(30)
C(5)	220(40)	110(30)	310(40)	-10(30)	30(30)	20(30)
C(6)	170(30)	110(30)	360(40)	20(30)	-20(30)	70(30)
C(7)	280(40)	230(30)	170(40)	10(30)	-40(30)	-20(30)
C(8)	250(40)	330(40)	510(50)	-50(30)	10(40)	140(30)
C(9)	290(40)	350(40)	510(50)	-270(30)	-160(40)	50(30)
C(10)	470(50)	360(40)	300(40)	-120(30)	-180(40)	-110(40)
C(11)	440(40)	230(30)	150(40)	-60(30)	-30(30)	-20(30)
C(12)	290(40)	220(30)	170(40)	60(30)	10(30)	-30(30)
C(13)	270(40)	180(30)	180(40)	-100(30)	40(30)	20(30)
C(14)	370(40)	210(30)	180(40)	30(30)	-40(30)	70(30)
C(15)	370(40)	240(30)	260(40)	60(30)	40(40)	10(30)
C(16)	260(40)	280(30)	340(40)	140(30)	150(30)	-20(30)
C(17)	170(30)	280(30)	310(40)	-30(30)	0(30)	10(30)
C(18)	290(40)	130(30)	140(40)	-10(20)	10(30)	20(30)
C(19)	170(30)	220(30)	180(40)	-40(30)	20(30)	-20(30)
C(20)	350(40)	230(30)	210(40)	-10(30)	40(30)	-10(30)
C(21)	450(40)	230(30)	330(50)	-90(30)	30(40)	20(30)
C(22)	470(50)	430(40)	230(40)	-90(30)	150(40)	-10(40)
C(23)	370(40)	250(30)	280(40)	40(30)	100(30)	-20(30)
C(24)	210(40)	200(30)	220(40)	-90(30)	20(30)	-20(30)
C(25)	220(40)	160(30)	180(40)	0(30)	10(30)	-30(30)
C(26)	170(40)	190(30)	300(40)	-20(30)	10(30)	-50(30)
C(27)	260(40)	220(30)	220(40)	-30(30)	80(30)	-60(30)
C(28)	310(40)	210(30)	180(40)	40(30)	10(30)	-40(30)
C(29)	630(50)	140(30)	210(40)	-10(30)	150(40)	90(30)
C(30)	960(60)	330(40)	300(50)	-30(30)	320(40)	30(40)
C(31)	1160(70)	140(30)	640(60)	-170(40)	360(50)	90(40)
C(32)	730(50)	190(30)	400(50)	90(30)	210(40)	-40(40)
C(33)	240(40)	160(30)	160(40)	20(30)	10(30)	-30(30)
C(34)	360(40)	200(30)	240(40)	10(30)	20(30)	-90(30)
C(35)	490(50)	340(40)	120(40)	-20(30)	-10(30)	80(30)
C(36)	400(50)	240(30)	370(50)	40(30)	180(40)	-10(30)
C(37)	310(40)	260(30)	170(40)	0(30)	50(30)	10(30)
C(38)	270(40)	200(30)	260(40)	90(30)	30(30)	0(30)
C(39)	230(40)	350(40)	250(40)	20(30)	0(30)	-20(30)
C(40)	280(40)	470(40)	370(50)	50(30)	-90(40)	-20(40)
C(41)	150(40)	460(40)	790(60)	100(40)	-40(40)	90(30)
C(42)	300(40)	330(40)	690(60)	-70(40)	130(40)	80(30)
C(43)	220(40)	240(30)	210(40)	-100(30)	-80(30)	10(30)
C(44)	280(40)	240(30)	220(40)	60(30)	-50(30)	-80(30)
C(45)	340(40)	250(30)	230(40)	-160(30)	-40(30)	40(30)
C(46)	270(40)	340(40)	140(40)	0(30)	70(30)	-20(30)
C(47)	300(40)	240(30)	120(40)	-60(30)	30(30)	-30(30)
C(48)	380(40)	220(30)	150(40)	10(30)	50(30)	70(30)
C(49)	360(40)	300(30)	290(40)	70(30)	10(40)	-70(30)
C(50)	560(50)	330(40)	330(50)	180(30)	170(40)	80(40)
C(51)	430(50)	460(40)	230(40)	30(30)	-60(40)	180(40)
C(52)	390(40)	330(40)	170(40)	70(30)	10(30)	50(30)
C(53)	300(40)	140(30)	150(40)	0(30)	10(30)	-10(30)
C(54)	260(40)	270(30)	300(40)	-60(30)	70(30)	-30(30)
C(55)	260(40)	310(40)	440(50)	-70(30)	120(40)	-20(30)

C(56)	220(40)	240(30)	500(50)	-40(30)	20(40)	-80(30)
C(57)	400(40)	140(30)	310(40)	-30(30)	10(40)	-50(30)
C(58)	300(40)	270(40)	210(40)	80(30)	20(30)	70(30)
C(59)	380(40)	260(30)	470(50)	0(30)	-100(40)	20(30)
C(60)	380(50)	300(40)	490(60)	-180(40)	-30(40)	130(40)
C(61)	950(70)	350(40)	1270(80)	20(40)	440(60)	330(40)

References

- (1) X. L. Feng, J. S. Wu, V. Enkelmann, K. Mullen, *Org. Lett.* **2006**, *8*, 1145.
- (2) K. Kambe, *J. Phys. Soc. Jpn.* **1950**, *5*, 48.
- (3) F. E. Mabbs and D. J. Machin, *Magnetism and Transition Metal Complexes*, Dover Publications, Inc., Mineola, 2008.
- (4) SQUEEZE - Sluis, P. v.d.; Spek, A. L. *Acta Crystallogr., Sect A* 1990, *46*, 194-201.